




# The insertase YidC chaperones the polytopic membrane protein MelB inserting and folding simultaneously from both termini

## Journal Article

### Author(s):

Blaimschein, Nina ; Parameswaran, Hariharan; Nagler, Gisela; Manioglu, Selen; Helenius, Jonne ; Ardelean, Cristian; Kuhn, Andreas; Guan, Lan; Müller, Daniel J. 

### Publication date:

2023-11-02

### Permanent link:

<https://doi.org/10.3929/ethz-b-000640073>

### Rights / license:

[Creative Commons Attribution 4.0 International](#)

### Originally published in:

Structure 31(11), <https://doi.org/10.1016/j.str.2023.08.012>

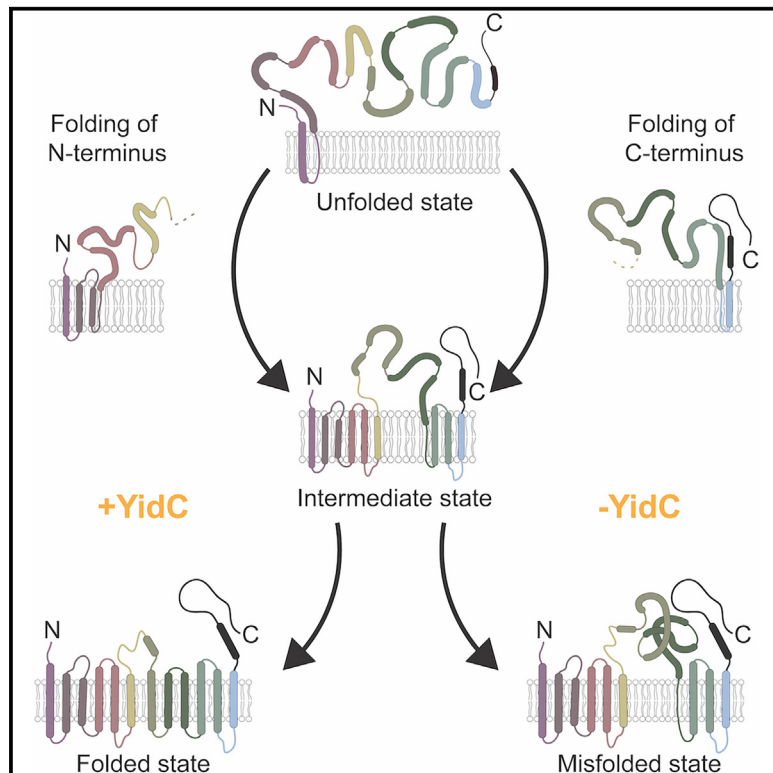
### Funding acknowledgement:

182587 - Characterizing the cell cycle dependent regulation of adhesion to extracellular matrix proteins (SNF)

# Structure

## The insertase YidC chaperones the polytopic membrane protein MelB inserting and folding simultaneously from both termini

### Graphical abstract



### Authors

Nina Blaimschein,  
 Hariharan Parameswaran,  
 Gisela Nagler, ..., Andreas Kuhn,  
 Lan Guan, Daniel J. Müller

### Correspondence

daniel.mueller@bsse.ethz.ch

### In brief

Blaimschein et al. monitors the folding pathways of single melibiose permeases MelB into the membrane. MelB itself forms two folding cores from which it stepwise inserts and folds into the membrane. However, this self-insertion process is prone to misfolding. It is observed how YidC accelerates and chaperones this folding process.

### Highlights

- YidC chaperones membrane insertion of MelB *in vivo* and *in vitro*
- MelB forms two folding cores related to its structural symmetry
- Misfolding dominates in the structural region interfacing both folding cores
- YidC chaperones weakly hydrophobic structural segments interfacing the folding cores



## Article

# The insertase YidC chaperones the polytopic membrane protein MelB inserting and folding simultaneously from both termini

Nina Blaimschein,<sup>1</sup> Hariharan Parameswaran,<sup>2</sup> Gisela Nagler,<sup>3</sup> Selen Manioglu,<sup>1</sup> Jonne Helenius,<sup>1</sup> Cristian Ardelean,<sup>4,5</sup> Andreas Kuhn,<sup>3</sup> Lan Guan,<sup>2</sup> and Daniel J. Müller<sup>1,6,\*</sup>

<sup>1</sup>Department of Biosystems Science and Engineering, Eidgenössische Technische Hochschule (ETH) Zürich, 4058 Basel, Basel-Stadt, Switzerland

<sup>2</sup>Department of Cell Physiology and Molecular Biophysics, Texas Tech University Health Sciences Center, Lubbock, TX 79430, USA

<sup>3</sup>Institute of Biology, University of Hohenheim, 70599 Stuttgart, Baden-Württemberg, Germany

<sup>4</sup>Basel, Basel, Switzerland

<sup>5</sup>Independent programmer

<sup>6</sup>Lead contact

\*Correspondence: [daniel.mueller@bsse.ethz.ch](mailto:daniel.mueller@bsse.ethz.ch)

<https://doi.org/10.1016/j.str.2023.08.012>

## SUMMARY

The insertion and folding of proteins into membranes is crucial for cell viability. Yet, the detailed contributions of insertases remain elusive. Here, we monitor how the insertase YidC guides the folding of the polytopic melibiose permease MelB into membranes. *In vivo* experiments using conditionally depleted *E. coli* strains show that MelB can insert in the absence of SecYEG if YidC resides in the cytoplasmic membrane. *In vitro* single-molecule force spectroscopy reveals that the MelB substrate itself forms two folding cores from which structural segments insert stepwise into the membrane. However, misfolding dominates, particularly in structural regions that interface the pseudo-symmetric  $\alpha$ -helical domains of MelB. Here, YidC takes an important role in accelerating and chaperoning the stepwise insertion and folding process of both MelB folding cores. Our findings reveal a great flexibility of the chaperoning and insertase activity of YidC in the multifaceted folding processes of complex polytopic membrane proteins.

## INTRODUCTION

Membrane protein biogenesis is essential for cell viability.<sup>1</sup> In bacteria, the highly conserved SecYEG and YidC pathways facilitate the insertion and folding of membrane proteins into the cytoplasmic cell membrane.<sup>2–4</sup> The Sec translocon, consisting of the subunits SecY, SecE, and SecG, together with accessory proteins, forms a multi-protein complex called the holo-translocon, which inserts polytopic membrane proteins into the cytoplasmic membrane.<sup>5,6</sup> YidC can act as part of the Sec holo-translocon or independently to facilitate the insertion and folding of mostly smaller, single- or double-spanning membrane proteins.<sup>7,8</sup> Interestingly, YidC has also been shown to promote the insertion and folding of the much more complex polytopic membrane protein lactose permease LacY.<sup>9–11</sup>

YidC is an essential cellular insertase and chaperone having highly conserved homologues in all kingdoms of life.<sup>12,13</sup> Furthermore, YidC protein sequences in Gram-negative bacteria share high similarities of up to 99%.<sup>14</sup> The crystal structure of YidC revealed a coiled-coil domain in the cytoplasmic loop C1 and five core transmembrane  $\alpha$ -helices forming a hydrophilic groove that opens toward the cytoplasm and reaches halfway through the lipid bilayer.<sup>15</sup> During the insertion process, the

nascent amino-terminal hydrophilic segment initially binds to the cytoplasmic loop C1 from which it is guided to the hydrophilic groove.<sup>16</sup> This groove can accommodate hydrophilic segments of the nascent polypeptide for their translocation through the lipid membrane,<sup>17</sup> while the hydrophobic transmembrane  $\alpha$ -helices of the substrate interact with the so-called greasy slide comprised of transmembrane  $\alpha$ -helices III and V of YidC to eventually insert into the membrane.<sup>18</sup> However, how YidC supports the insertion and folding of larger polytopic membrane proteins remains to be fully understood.

Studying the folding processes of membrane proteins at the single-molecule level remains a challenge in molecular biology despite their importance to understand the link between tertiary structure and function. Many biophysical studies involve chemical or thermal denaturation to study these processes, which do not consider important physiological factors, such as membrane, buffer solution or temperature relevant to protein folding.<sup>19–21</sup> Atomic force microscopy (AFM)-based single-molecule force spectroscopy (SMFS) has proven to be a versatile tool for monitoring the insertion and folding process of individual structural segments into native or synthetic membranes until a membrane protein has been folded.<sup>9,22–25</sup> Furthermore, the insertion and folding of membrane proteins can be studied in



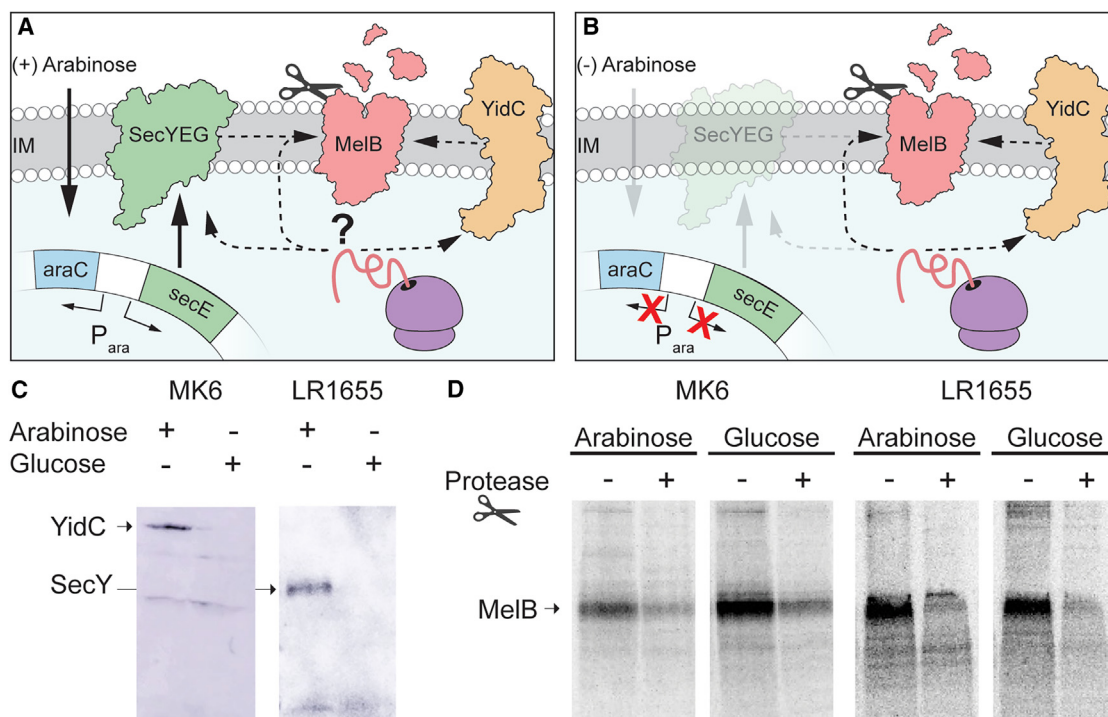


**Figure 1. Insertion of MelB into the cell membrane in the presence of YidC and in the absence of SecYEG**

(A and B) Schematics of experimental design in the conditionally SecYEG-depleted *E. coli* strain LR1655. (A) In the presence of arabinose, SecE is expressed and, thus, SecYEG (green) is present in the inner membrane (IM) whereas the chromosomally encoded YidC (orange) is not affected by arabinose.<sup>54</sup> From the ribosome (purple) newly synthesized MelB (red) is inserted into the inner membrane via an unknown pathway. As soon as inserted into the membrane, the radioactively pulse-labeled MelB can be cleaved by the externally added protease K (scissors). (B) In the *E. coli* strain LR1655 SecE is not expressed in the absence of arabinose and thus SecYEG is not detectable in the IM. Depletion of SecE leads to a rapid loss of SecY and consequently the SecYEG complex.<sup>55</sup> Because radioactively pulse-labeled MelB is digestible by externally added proteinase K this demonstrates the successful membrane insertion of MelB in the absence of SecYEG and in the presence of YidC. The schematics work analogously for the YidC-depleted *E. coli* strain MK6.

(C) Western blot of YidC in the MK6 strain and SecY in the LR1655 strain showing a complete depletion of insertase or translocase, respectively, after substitution of arabinose with glucose during bacterial growth.

(D) Radioactively pulse-labeled MelB isolated by immunoprecipitation and separated by SDS-PAGE. In the absence of YidC (MK6, glucose) or SecYEG (LR1655, glucose), MelB is present in the IM and digestible by the protease K (scissors).

great mechanistic detail in the presence of insertases and chaperones such as YidC. Previous studies on lactose permease LacY provided a first insight into how SecYEG and YidC guide the folding process of a polytopic inner membrane protein.<sup>9,10,26</sup> However, further investigations are needed on other polytopic inner membrane proteins to conclude which part of the described folding process is intrinsic to the membrane protein or to the insertase.

Here, we investigate the insertion and folding process of the melibiose permease MelB of *Salmonella typhimurium* in the presence and absence of YidC *in vivo* and *in vitro*. MelB is a prototype for the major facilitator superfamily (MFS) and exhibits the typical MFS-fold.<sup>27,28</sup> Structurally, 12 transmembrane  $\alpha$ -helices are organized into two pseudo-symmetric  $\alpha$ -helical bundles, which are connected by a 31 amino acid (aa) long cytoplasmic middle-loop C3. Usually, polytopic membrane proteins require SecYEG to insert into the cytoplasmic membrane.<sup>29</sup> However, using a conditionally depleted SecYEG *Escherichia coli* strain in combination with protease mapping, we find that MelB can be inserted into the cell membrane in the presence of YidC and absence of SecYEG. To further

investigate this phenomenon, we use SMFS to mechanically unfold MelB partially and let the unfolded MelB polypeptide insert and fold into the membrane in the absence and presence of YidC. We find that the pseudo-symmetric  $\alpha$ -helical bundles of MelB form two independent folding cores, which cannot complete folding in the absence of YidC because the structural regions that interface both cores show a high probability of misfolding. YidC assists in this rather complex insertion and folding process by chaperoning and accelerating the individual insertion and folding steps and by inserting and folding the weakly hydrophobic structural elements that connect the two bundles of the transporter.

## RESULTS

### MelB can insert into cell membranes in the absence of SecYEG if YidC is present

Using protease mapping,<sup>30</sup> we investigated whether MelB requires the SecYEG translocase or/and the YidC insertase to insert and fold into the cytoplasmic membrane of *E. coli* (Figures 1A and 1B). The plasmid pK95 encoding His-tagged

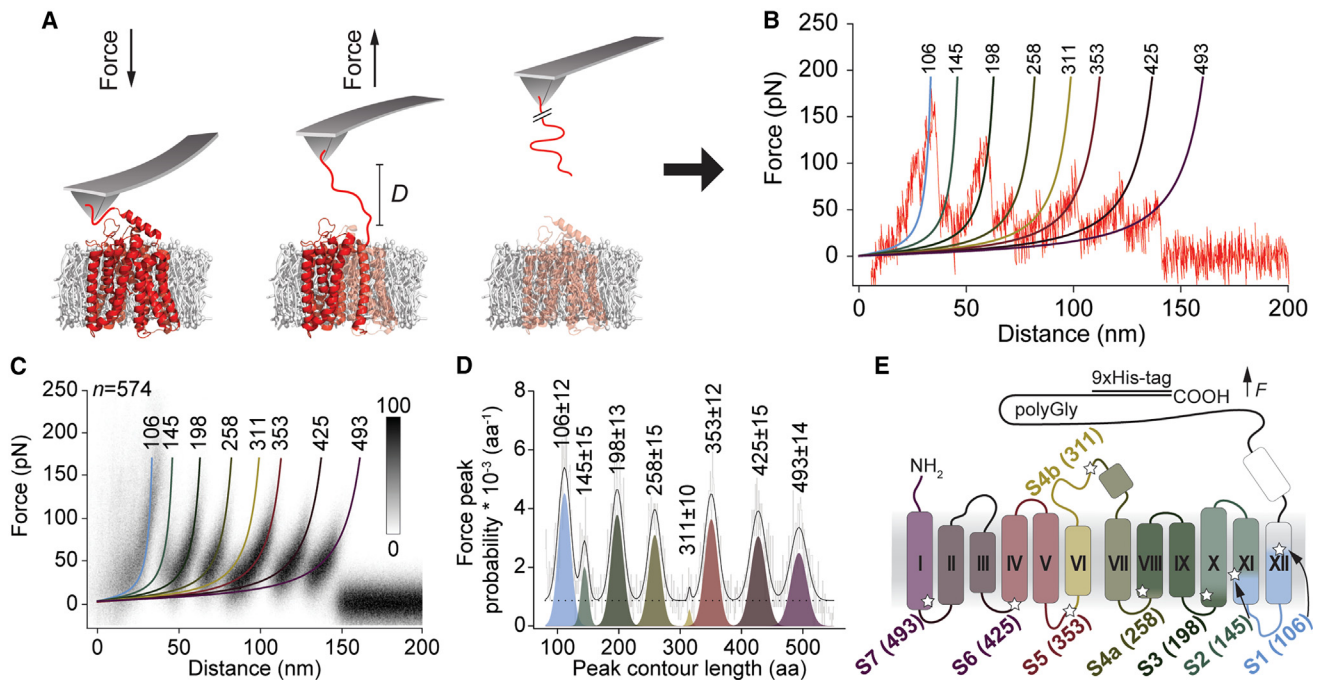


**Figure 2. Force peak pattern reveals the mechanical unfolding intermediates of natively folded MelB**

(A) Schematics of the mechanical unfolding of a single MelB (red, PDB 7L17) from the *E. coli* polar lipid membrane using SMFS. The tip of the AFM cantilever is pushed onto MelB with a force of 700 pN for 0.5 s to promote the unspecific attachment of the elongated polyGly C-terminal end to the tip. The cantilever tip is then retracted until MelB is fully unfolded and finally extracted from the lipid membrane.

(B) Characteristic force-distance curve recorded upon mechanically unfolding MelB from the lipid membrane in SMFS buffer solution (20 mM Tris-HCl, pH 7.5, 20 mM melibiose, 100 mM NaCl) and at  $\approx 25^\circ\text{C}$ . Each force peak was fitted with the worm-like chain (WLC) model (STAR Methods) to reveal the mean contour length given in amino acids (aa) at the top of each WLC curve.

(C) The superposition of 574 force-distance curves shows the characteristic force peak pattern recorded upon the mechanical unfolding of MelB. WLC fit and mean contour length is given for each force peak.

(D) Histogram of unfolding force peaks fitted with a Gaussian mixture model. Each differently colored force peak is labeled with the mean contour length and standard deviation in aa.

(E) Mapping of structural segments S1–S7 that stabilize MelB against mechanical unfolding. The appearance of the force peak at aa 311, which depends on the presence of MelB substrates, is  $\approx 6\%$  in the buffer solution (20 mM Tris-HCl, pH 7.5, 100 mM NaCl, 20 mM melibiose) used.<sup>32</sup> Due to the varying detection probability, the corresponding structural segment was labeled as S4b. The coloring of the structural segments corresponds to the unfolding force peaks shown in (D). Each white star localizes the contour length of the corresponding force peak (aa numbers in brackets), counted from the mechanically unfolded C-terminal end. Labeled are transmembrane  $\alpha$ -helices I–XII, the 42 aa long polyglycine (polyGly) extension [GSM(G<sub>11</sub>)EAVEEEAVEEEA(G<sub>11</sub>)S], and the 9xHis-tag.

MelB was transformed into *E. coli* strains MK6 and LR1655 that can be depleted for YidC and SecE, respectively. In both strains an arabinose-controlled promoter led to the complete depletion of either YidC or SecYEG after 3 h of growth (Figure 1C). At this point, the cells were pulse-labeled for 3 min with <sup>35</sup>S-methionine, converted to spheroplasts, and treated with protease K (Figure 1D). MelB was visualized by phosphorimaging after immunoprecipitation. In YidC-depleted MK6 cells and in SecYEG-depleted LR1655 cells, the radioactively labeled MelB was essentially digested by protease to the extent observed under non-depleted conditions. Testing MelB insertion in the absence of both YidC and SecYEG was unsuccessful because *E. coli* is not viable if it lacks both chaperones. Therefore, we conclude that MelB can insert into the cytoplasmic membrane of *E. coli* in the presence of YidC and in the absence of SecYEG, or in the presence of SecYEG and in the absence of YidC. Thus, the presence of either YidC or SecYEG is sufficient to insert MelB into the cell membrane.<sup>31</sup>

### The mechanical unfolding pathway of MelB shows a characteristic force peak pattern

To assess how YidC assists MelB in inserting and folding into the lipid membrane, we first characterized the mechanical unfolding pattern of natively folded MelB by SMFS. For this, we purified and reconstituted MelB into *E. coli* polar lipid membrane (Figure S1A). After having adsorbed the MelB proteoliposomes on mica and localizing the MelB membranes in buffer solution by AFM (Figure S1B), we gently pushed the tip of the AFM cantilever (700 pN for 0.5 s) onto a membrane patch to promote the unspecific attachment of the MelB polypeptide (Figure 2A). To increase the probability of attaching the C-terminal end, MelB had been elongated by an unstructured 42 aa sequence.<sup>32</sup> Upon retraction of the AFM cantilever, the C-terminal polypeptide was mechanically stretched, thereby forcing MelB to unfold stepwise. This mechanical unfolding of MelB was recorded as a force-distance curve (Figure 2B).<sup>33</sup> To reveal the contour length of the polypeptide stretches unfolded in each unfolding step, we fitted each force peak using the worm-like-chain (WLC) model.<sup>34</sup> Repeating

this procedure multiple times revealed a reproducible sawtooth-like force peak pattern of the force-distance curves with up to eight force peaks (Figures 2C and 2D).<sup>32</sup> Each force peak within the force peak pattern describes the unfolding of a structural segment that stabilizes MelB against the mechanical unfolding from the C-terminal end (Figure 2E). The sequence of force peaks in such a force peak pattern thus describes the unfolding intermediates that a membrane protein takes along its mechanical unfolding pathway.<sup>35</sup> For MelB, we detected eight structural segments S1, S2, S3, S4a, S4b, S5, S6, and S7, which describe eight unfolding intermediates that the transporter takes upon transiting from the natively folded state to the fully unfolded state. It has been shown that such unfolding force peak patterns of polytopic membrane proteins are sensitive to ligand-binding, lipid composition, functional state, mutations, fold, and supramolecular assembly.<sup>32,36–41</sup> Along this line, the probability of detecting the force peak at aa 311 that corresponds to structural segment S4b has been shown to depend on the presence of MelB substrates (e.g., sugar, cation) and is  $\approx 6\%$  in the buffer solution (20 mM Tris-HCl, pH 7.5, 100 mM NaCl, 20 mM melibiose) used here.<sup>32</sup> Taken together, the observed well-defined and reproducible force peak pattern, thus, describes the mechanical unfolding steps and pathway of natively folded MelB.

#### Fully unfolded MelB cannot insert into the lipid membrane by itself or in the presence of YidC

Next, we wanted to investigate whether the fully unfolded and extracted MelB polypeptide can self-insert into the lipid membrane in the absence or presence of YidC. Therefore, we co-reconstituted YidC and MelB into *E. coli* polar lipid membrane. YidC homologues in Gram-negative bacteria have very high sequence similarity, which is  $\approx 95\%$  between YidC from *E. coli* and *S. typhimurium* (Figure S2, STAR Methods). MelB and YidC were co-reconstituted in an equimolar ratio of 1:1. The successful co-reconstitution was confirmed by SDS-PAGE and AFM imaging (Figures S1A and S1C). SMFS unfolding experiments showed the co-reconstitution and native fold of MelB and YidC, and that MelB and YidC distributed in close proximity in the membrane (Figure S3). Furthermore, membrane proteins, although adsorbed to mica, can diffuse within the membrane.<sup>42,43</sup> Thus, we can conclude that both co-reconstituted MelB and YidC are present in the lipid membrane, show their native fold, and are in sufficient proximity to eventually interact.

Next, the cantilever tip was pushed onto the membrane to unspecifically attach the C-terminal end of a single MelB and to mechanically unfold and extract the MelB polypeptide from the membrane (Figures 3A and 3B). In principle, this attachment allowed the N-terminal end of the fully unfolded MelB polypeptide to freely insert and fold into the membrane, which is also the case during cytoplasmic membrane protein biogenesis.<sup>1</sup> The mechanically unfolded and extracted MelB polypeptide was then brought and kept in close proximity to the membrane ( $\approx 10$  nm). The distance between the cantilever tip and the membrane ensured that the tip could not contact and attach to other MelBs that reside in the membrane. After allowing the unfolded polypeptide to interact with the membrane for 2 s, we term this time frame folding time, the AFM cantilever was fully retracted and a force-distance curve was recorded. This second force-distance curve was analyzed to detect whether the MelB poly-

peptide inserted and folded into the membrane. From 142 initially unfolded MelB transporters, only a few force-distance curves recorded force peaks during the second retraction. However, these force peaks did not match the force peaks observed for the correctly inserted and folded structural segments of natively folded MelB. Consequently, these force peaks indicate that the unfolded polypeptide has adopted stable interactions with the membrane surface, misfolded outside the membrane, or inserted itself into the membrane and adopted non-native conformations. Subsequently, such events were interpreted as misfolded states of the MelB polypeptide.

To further test whether YidC assists MelB insertion into the lipid membrane, we repeated the experiment with the co-reconstituted MelB and YidC sample (Figure 3C). After a folding time of 2 s, none of the force-distance curves recorded from 785 initially fully unfolded MelB transporters showed force peaks that could be assigned to the characteristic force peak pattern of natively folded MelB. Thus, we conclude that in our *in vitro* experiments the fully unfolded and extracted MelB polypeptide cannot insert and fold into the lipid membrane without or with the help of the YidC insertase. In view of our *in vivo* experiments mentioned before in *E. coli*, one could speculate that *in vivo* YidC is assisted by other molecules (e.g., chaperones or membrane proteins) to insert and fold MelB into the cytoplasmic membrane. However, which molecules co-assist in this insertion and folding process remain to be shown.

#### N-terminal segments of partially unfolded MelB remain stably embedded in the lipid membrane

Having learned that in our *in vitro* experiment the fully unfolded and extracted MelB polypeptide cannot insert into the lipid membrane without the help of other molecules of the cellular machinery, we tested whether the MelB polypeptide can insert and fold into the lipid membrane once the initial insertion step has been overcome. For these experiments, we partially unfolded MelB, leaving the last N-terminal structural segment(s) embedded in the membrane. This state mimics the first step of membrane protein insertion *in vivo*.<sup>44,45</sup> To address this question, we first investigated whether the N-terminal structural segments that remain embedded in the lipid membrane undergo significant changes. Thereto, we partially unfolded MelB from the membrane by mechanically pulling the C-terminus at varying distances of 70, 100, or 130 nm (Figures 4A, 4B, and S4). Thus, these partial unfoldings left different portions of the N-terminal domain of MelB folded in the membrane. Subsequently, we reapproached the AFM cantilever to close proximity of the membrane ( $\approx 10$  nm), where we kept the partially unfolded MelB polypeptide for 2 s. Then, the AFM cantilever was fully retracted to fully unfold and extract MelB from the membrane. The force peaks recorded during this second retraction were compared with the force peaks recorded of the natively folded MelB. Independent of the extent to which MelB has been partially unfolded in the first step, in the second retraction, we recorded the force peaks of the structural segments that were left in the membrane after the first partial unfolding of MelB. These force peaks showed positions identical to those observed for the unfolding of the natively folded MelB. However, in some cases we detected additional force peaks of structural segments that had already unfolded. These additional force peaks occurred at the same positions

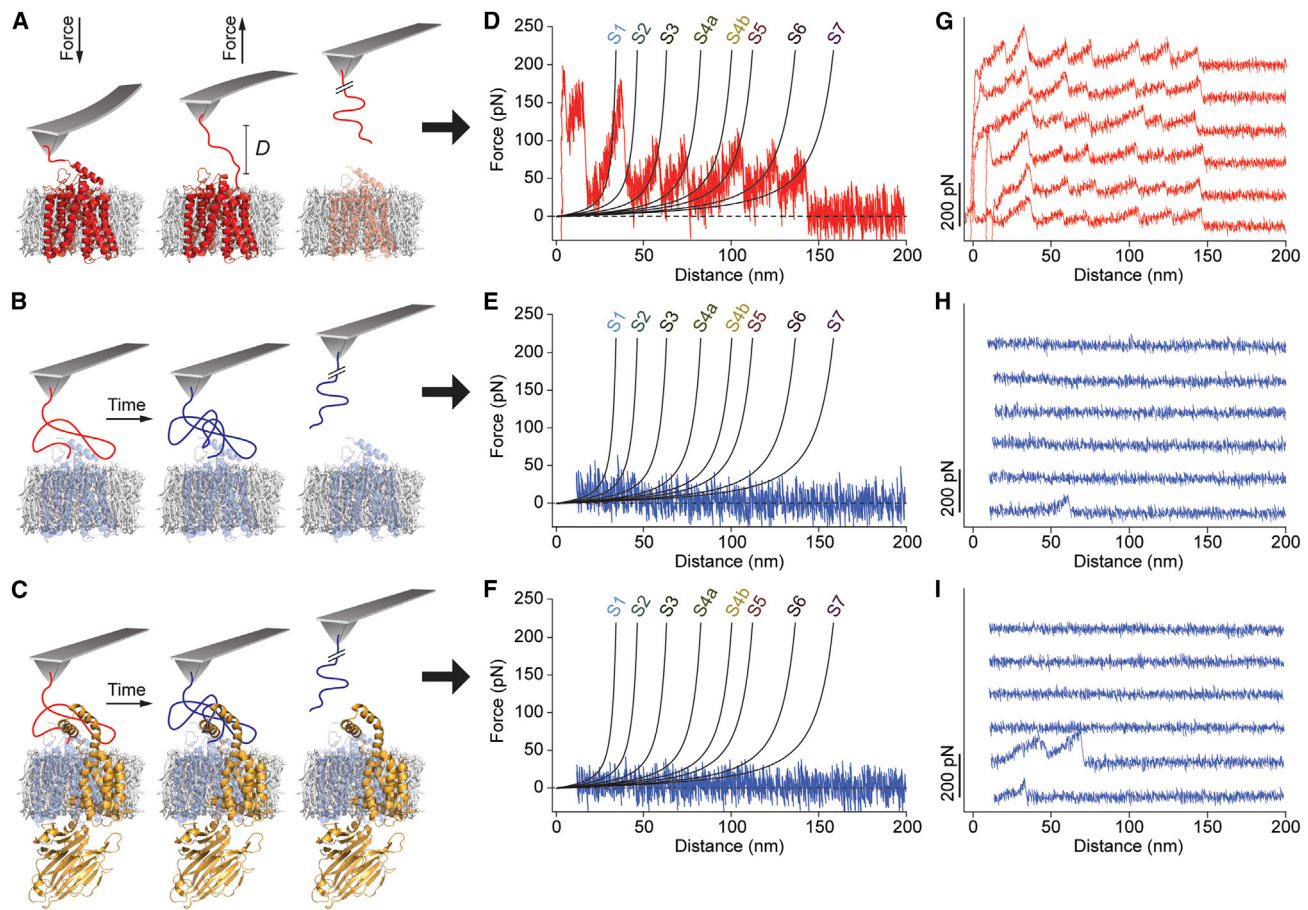


**Figure 3. SMFS insertion and folding experiments of the completely unfolded and extracted MelB polypeptide in the lipid membrane in the absence and presence of YidC**

(A) Schematic representation of the complete unfolding and extraction of a natively folded MelB from the *E. coli* polar lipid membrane as described (Figure 2A). To unspecifically attach the elongated polyGly C-terminal end of MelB, the cantilever tip is pushed onto the MelB membrane with a force of 700 pN for 0.5 s. Upon subsequent retraction of the AFM cantilever, the attached polypeptide mechanically stretches, and MelB unfolds stepwise until it is completely unfolded and extracted from the membrane.

(B and C) The fully extracted MelB polypeptide is lowered to the membrane at a different lateral position and at a vertical distance of  $\approx 10$  nm. After the polypeptide is given time to interact and/or reinsert into the lipid membrane, the AFM stylus is retracted and a force-distance curve recorded. The force-distance curve is analyzed for the insertion and folding of the MelB polypeptide into structural segments such as observed for natively folded MelB. The insertion and folding experiments of the completely unfolded and extracted MelB polypeptide were performed (B) in the absence and (C) in the presence of YidC (orange).

(D–F) Each retraction of the AFM cantilever is recorded as a force-distance curve. The black curves depict the characteristic WLC curves fitting the characteristic force peak pattern of natively folded MelB and are labeled with the corresponding structural segment S1–S7 (Figure 2). (D) The red force-distance curve represents the characteristic sawtooth-like force peak pattern recorded upon the mechanical unfolding of native MelB.

(E and F) The blue force-distance curves, which are recorded from the second retraction of the AFM cantilever, show no force peaks.

(G–I) Exemplary force-distance curves for the (G) mechanical unfolding of natively folded MelB (red) and (H and I) force-distance curves (blue) recorded after a specified folding time in the (H) absence or (I) presence of YidC. Experiments were carried out in SMFS buffer solution (20 mM Tris-HCl, pH 7.5, 20 mM melibiose, 100 mM NaCl) and at  $\approx 25^\circ\text{C}$ .

as detected upon the unfolding of natively folded MelB. From this we conclude that the structural segments of the partially unfolded MelB transporter remain stably folded in the membrane within the time frame of 2 s.

### YidC reduces misfolding and supports the insertion and folding of MelB

Our previous observation shows that the N-terminal end of the partially unfolded MelB polypeptide remains stably inserted in the membrane and that the unfolded polypeptide established force peaks, which correlate to that of natively folded MelB.

This observation indicates that the partially unfolded polypeptide can insert and fold structural segments into the membrane. Thus, we wanted to characterize the folding and insertion process of the partially unfolded MelB polypeptide closer in the absence and presence of YidC. Therefore, we mechanically pulled the C-terminal end of MelB up to a distance of 130 nm, which unfolded the structural segments S1–S6 and left the last structural segment S7 embedded in the membrane (Figure 4). Then, we reapproached the AFM cantilever in close proximity to the membrane ( $\approx 10$  nm) where the unfolded polypeptide was allowed to relax, insert, and fold into the membrane for 0.5–5 s.

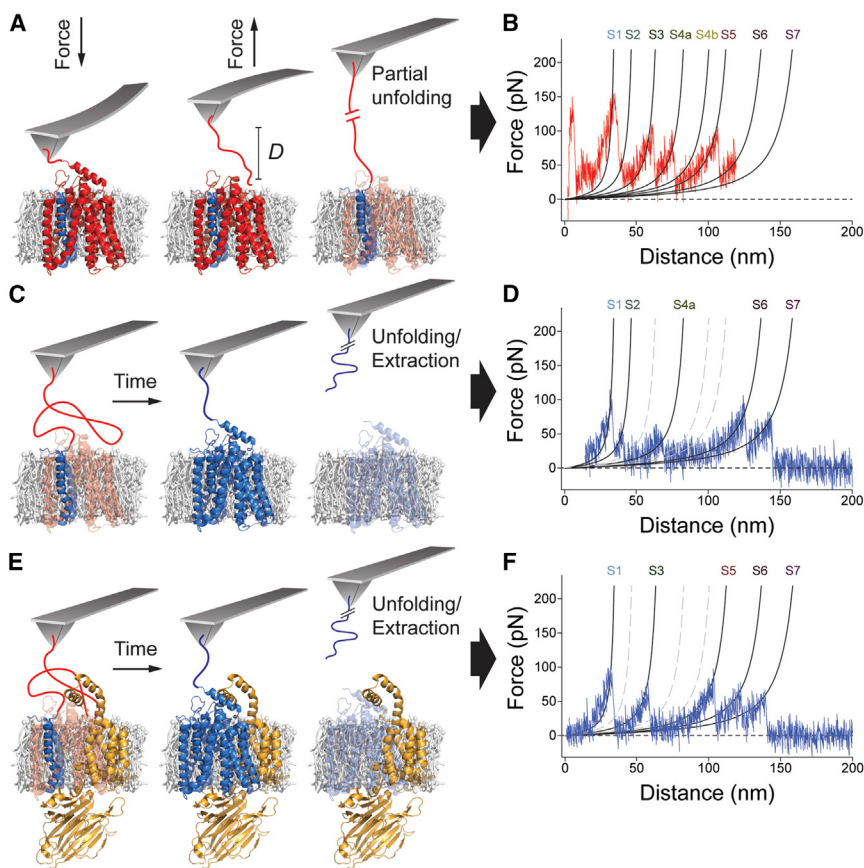


**Figure 4. SMFS insertion and folding experiments of the partially unfolded MelB in the absence and presence of YidC**

(A, C, and E) Schematics of the folding experiments. (A) The initial unfolding of natively folded MelB follows a similar procedure as the unfolding experiments described (Figure 2). The cantilever tip is gently pushed onto MelB (red, PDB 7L17) in the *E. coli* polar lipid membrane (gray) to unspecifically attach the elongated polyGly C-terminal end. Then, the tip is vertically retracted for only 130 nm to leave the last structural segment S7 of MelB (blue) embedded in the membrane. (B) During the limited retraction a force-distance curve records the characteristic unfolding force peak pattern of MelB, except that of structural segment S7, which remains embedded in the membrane. WLC fits (black curves) and structural segments (S1–S7) are given for each of the eight possible force peaks of natively folded MelB (C and E). After the partial unfolding of MelB, the cantilever tip is approached to the membrane surface where it is kept at a distance of  $\approx 10$  nm. At this position, the partially unfolded MelB polypeptide (blue) is given a specified time (0.5–5 s) to fold into the membrane (C) in the absence or (E) presence of YidC (orange). Subsequently, the cantilever tip is fully retracted to completely unfold and extract MelB from the membrane.

(D and F) The force peaks of the force-distance curve recorded during the second retraction provide information which structural segments of MelB inserted and folded into the membrane. WLC fits shown in (D and E) were taken from natively folded MelB (Figure 2). Black curves indicate WLC

fits of the force peaks detected for natively folded MelB and are each labeled with the respective structural segment S1–S7. Gray dashed WLC fits indicate missing force peaks.

After this folding time, the cantilever was retracted to fully unfold and extract MelB. We compared the force peak pattern recorded upon this second retraction with the characteristic force peak pattern recorded upon the mechanical unfolding of natively folded MelB. Each folding experiment was classified into one of three categories (Figure S5): (i) If the force-distance curve recorded only force peaks of structural segments S1–S6 of natively folded MelB, the polypeptide was considered to have correctly inserted and folded at least one or more structural segments. Thus, it was classified as folded. (ii) If the force-distance curve recorded at least one force peak that did not match the force peak pattern of natively folded MelB, the polypeptide must have adopted a non-native fold, and was classified as misfolded. (iii) If the force-distance curve did not record any force peaks within the pulling distance of  $\approx 130$  nm (i.e., structural segments S1–S6), the polypeptide was classified as having remained unfolded.

A first set of insertion and folding experiments, which we performed at four different folding times of 0.5, 1, 2, and 5 s, revealed a surprisingly high capability of partially unfolded MelB to insert and fold structural segments into the lipid membrane in the absence of YidC (Figure S6). After only 0.5 s  $80.2 \pm 6.1\%$  (average  $\pm$  SE,  $n = 130/162$ ) of the partially unfolded MelB polypeptide inserted and folded one or more structural segments such as detected for natively folded MelB. About  $9.3 \pm 4.5\%$  ( $n = 15/162$ ) of partially unfolded MelB misfolded, while the remaining  $10.5 \pm 4.7\%$  ( $n = 17/162$ ) remained unfolded (Figure 6A).

However, by increasing the folding time to 5 s the number of MelB polypeptides that correctly folded one or more structural segments decreased to  $57.6 \pm 12.6\%$  ( $n = 34/59$ ) while the number of MelB polypeptides showing at least one misfolding event increased to  $40.7 \pm 12.5\%$  ( $n = 24/59$ ). This trend has also been observed with the MFS transporter LacY<sup>9</sup> and is in agreement with the literature stating that hydrophobic structural segments, which cannot be inserted into the membrane and remain exposed to the hydrophilic environment, increase their probability of misfolding with time. Upon repeating our folding experiments of partially unfolded MelB in the presence of YidC (Figures 4E, 4F, and 5), we observed that the insertase suppressed the misfolding of the MelB polypeptide at higher folding times of 2 s and 5 s (Table S1). At each of the two latter folding times the misfolding probability of the MelB polypeptide was about 2-fold lower in the presence of YidC, thus highlighting the chaperoning effect of the insertase. Taken together, the results show that the MelB polypeptide with its N-terminal segments already being inserted in the membrane can itself insert and fold structural segments into the membrane, but that this process is hindered by misfolding events. In the presence of YidC these misfolding events are suppressed to background levels.

#### YidC increases the folding rate of MelB segments

To further explore the chaperoning effect of YidC, we analyzed the number of folded and misfolded structural



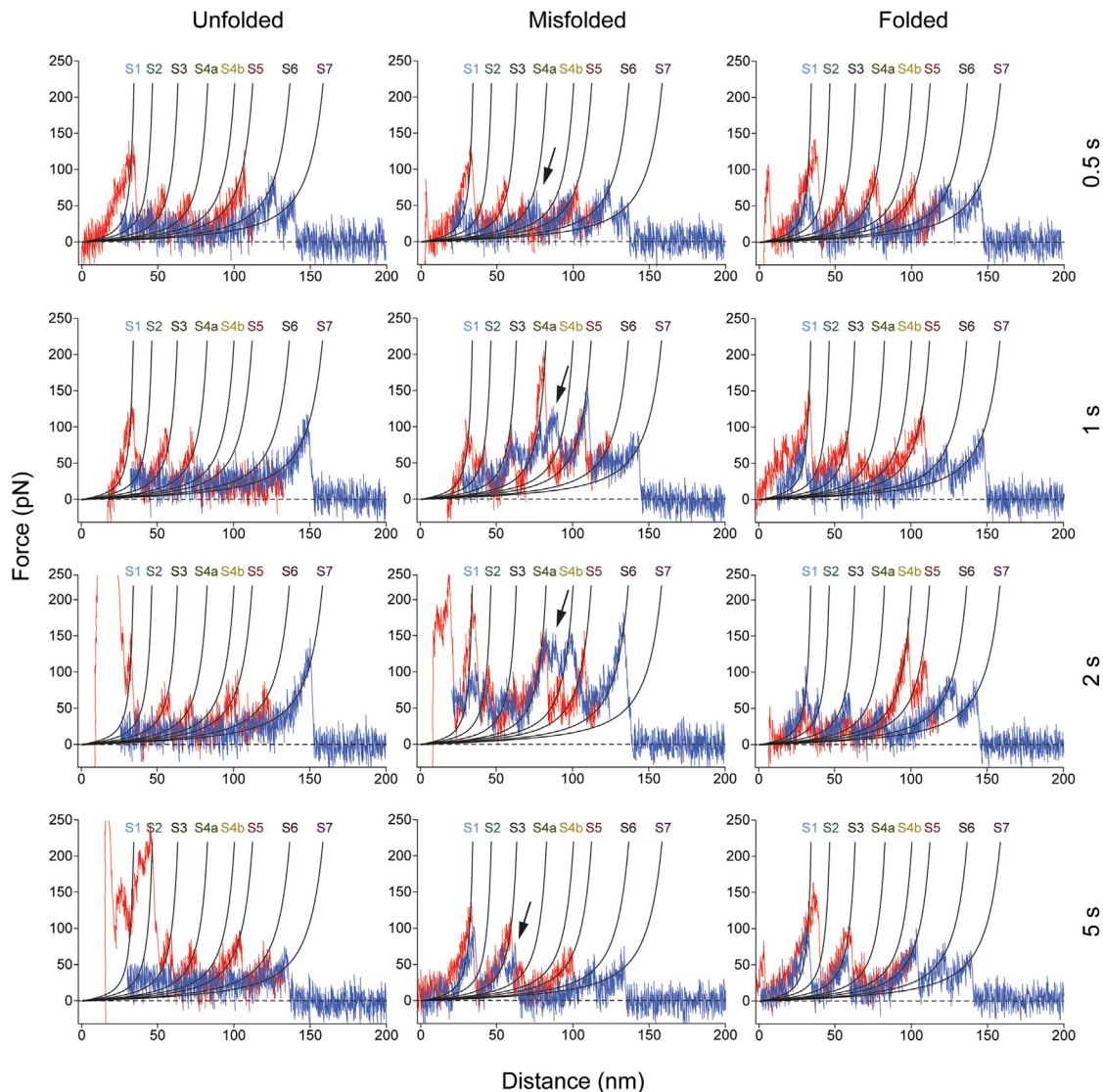


**Figure 5. Representative force-distance curves showing the insertion and folding of partially unfolded MelB in the presence of YidC**

Force-distance curves recording the initial partial unfolding of MelB are colored in red. Force-distance curves recording the full unfolding and extraction of the partially unfolded MelB after a given insertion and folding time are colored in blue. Insertion and folding experiments were conducted at 0.5, 1, 2, or 5 s and in the presence of YidC. The WLC curves were taken from the characteristic force peak pattern of native MelB and were labeled with the structural segments S1–S7 (Figure 2). Following the criteria described (Figure S5), the force-curves were classified “Unfolded,” “Misfolded,” or “Folded.” Black arrows indicate force peaks, which do not match the WLC curves (black lines) of native MelB, and thus indicate misfolding. SMFS experiments were performed in SMFS buffer solution (20 mM Tris-HCl, pH 7.5, 20 mM melibiose, 100 mM NaCl) and at  $\approx 25^{\circ}\text{C}$ . See also Figure S6.

segments at the folding times (Figures 6B and 6C; Table S2). In the absence of YidC, the MelB polypeptide inserted and folded approximately the same amount of  $3.8 \pm 0.2$  ( $n = 509$ ) structural segments for all folding times tested. Thus, the folding rate can be considered constant. On the other hand, the number of misfolded segments increased from  $1.3 \pm 0.1$  ( $n = 162$ ) at 0.5 s to  $2.3 \pm 0.2$  ( $n = 59$ ) at 5 s. Thus, with time, the misfolding rate of the MelB polypeptide increased. In contrast, in the presence of YidC, the number of misfolded segments essentially remained at low levels of  $1.4 \pm 0.1$  ( $n = 477$ ). Furthermore, YidC increased the number

of correctly inserted and folded structural segments of MelB from 4.5 at 0.5 s ( $n = 151$ ) to 5.5 at 5 s ( $n = 74$ ). The linear regression of folded segments over the folding time revealed an average folding rate of  $\approx 0.2$  structural segments per second (Figure 6D). From this we conclude that, in the absence of YidC, MelB increasingly misfolds over the course of measured folding times, possibly due to the stagnant folding rate of structural segments. YidC, on the other hand, increases the folding rate of structural segments and simultaneously decreases the probability that the MelB polypeptide will misfold.

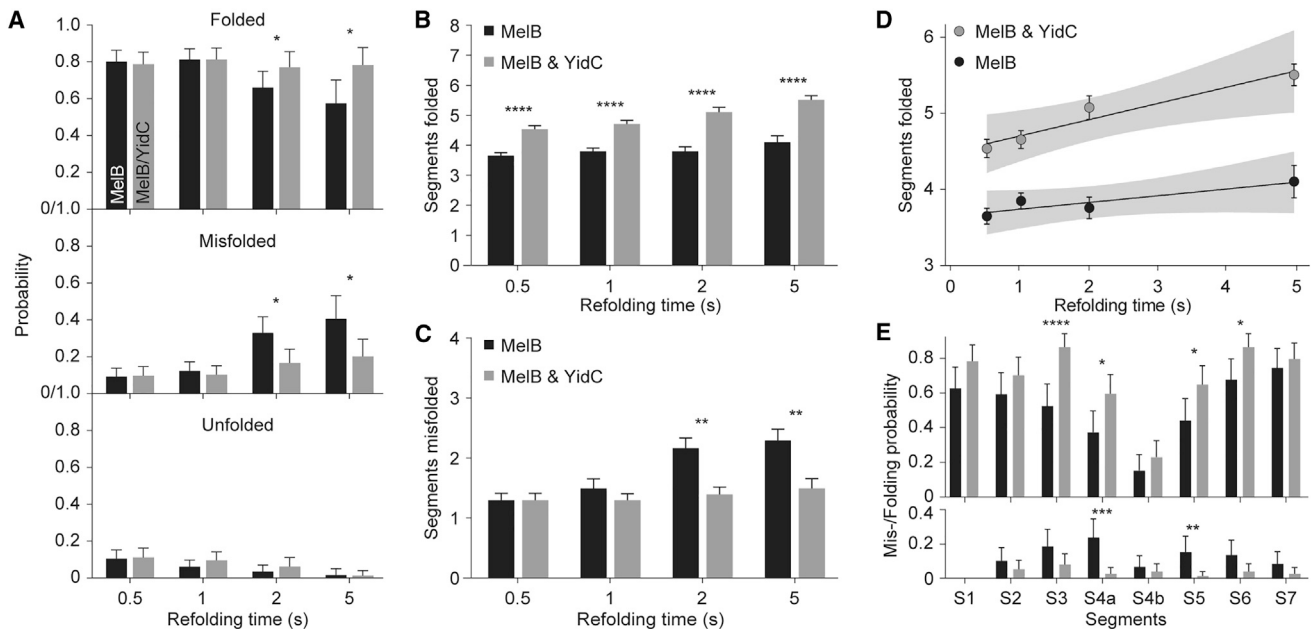


**Figure 6. Folding of partially unfolded MelB in the absence and presence of YidC**

(A) Probability of the partially unfolded MelB polypeptide to fold into the membrane, misfold, or remain unfolded in the absence (black;  $n = 162$  (0.5 s), 177 (1 s), 111 (2 s), 59 (5 s)) or presence (gray;  $n = 151$  (0.5 s), 156 (1 s), 96 (2 s), 74 (5 s)) of YidC. The data are given for four different folding times of 0.5, 1, 2, and 5 s. (B) Average number of folded structural segments per unfolded MelB at each folding time in the absence (black) and presence (gray) of YidC. (C) Average number of misfolded structural segments per partially unfolded MelB at each folding time in the absence (black) and presence (gray) of YidC. (D) Linear regression (fitted black line) of the average number of structural segments folded over the folding time. Within a confidence interval of 95% (gray shaded area) the folding rate of structural segments was  $0.09 \pm 0.03 \text{ s}^{-1}$  (average  $\pm$  SEM.) in absence of YidC and  $0.2 \pm 0.04 \text{ s}^{-1}$  (average  $\pm$  SEM) in presence of YidC. (E) Folding (top) and misfolding (bottom) probability of each structural segment S1–S7 of MelB at 5 s folding time in the absence (black) and presence (gray) of YidC. The folding probability is never expected to reach one, since the probability of detecting the mechanical unfolding of a structural segment of natively folded MelB is below one. For all data shown in this figure, the MelB polypeptide was partially unfolded for 130 nm to leave the structural segment S7 embedded in the membrane (Figure 4). Error bars, SEM (B–D) and SE (A and E).  $p$  values of the statistical analysis are given in Tables S1–S4. \* $p \leq 0.05$ , \*\* $p \leq 0.01$ , \*\*\* $p \leq 0.001$ , \*\*\*\* $p \leq 0.0001$ . See also Figure S7.

### YidC supports the folding of structural segments neighboring the middle-loop C3

To better understand how YidC increases the folding rate and prevents MelB from misfolding, we determined the folding and misfolding probabilities of each individual structural segment S1–S7 of MelB (Figures 6E and S7). Throughout all tested folding times and in the absence of YidC, the MelB polypeptide showed high probabilities of simultaneously inserting and folding segments from both terminal ends. For example, at 5 s folding time, the probabilities for the segments at the terminal ends S1, S2, S6, and S7 were  $63 \pm 12\%$ ,  $59 \pm 13\%$ ,  $68 \pm 12\%$ , and  $75 \pm 11\%$ , respectively (Figure 6E). This unexpected preference for insertion and folding is also observed in individual single-molecule experiments (Figures 4F, 5, and S6). However, the structural segments S3–S5 that interface the N- and C-terminal  $\alpha$ -helical bundles and include the 31 aa long cytoplasmic middle-loop C3 were less likely to fold with folding probabilities of  $53 \pm 13\%$  (S3),  $37 \pm 12\%$  (S4a),  $15 \pm 9\%$  (S4b), and  $44 \pm 13\%$  (S5) after 5 s folding time. In general, S4a showed the highest probability of misfolding (Figure 6E). This suggests that the two bundles insert and fold separately from each other and that this process progresses from the outmost terminal segments toward the middle-loop C3 that connects both domains. However, the insertion and folding process is interrupted because the

structural segments S3 and S4a show a high propensity to misfold. In the presence of YidC, both structural segments S3 and S4a considerably increased their folding probability and the misfolding probability of structural segments reduced to background levels (Figures 6E and S7; Tables S3 and S4). Interestingly, structural segment S4a harbors the weakly hydrophobic  $\alpha$ -helix VII. In general, structural segments neighboring the middle-loop C3 increased their probability of misfolding with time. YidC particularly prevents these segments from misfolding at longer time points and increases their probability of insertion and folding already within 0.5 s. Interestingly, the presence of YidC does not hinder the MelB polypeptide from simultaneously forming two insertion and folding cores of the C-terminal and N-terminal domains.

### DISCUSSION

Our study elucidates the role of the membrane insertase and chaperone YidC in assisting a member of the MFS, the melibiose permease MelB, to fold into the lipid membrane and compares the results with previous findings on the lactose permease LacY. During membrane protein biogenesis, the nascent polypeptide exits the ribosome with its N-terminal domain to insert and fold into the inner cell membrane.<sup>45</sup> Our *in vivo* experiments

show that MelB can insert into the cytoplasmic membrane in the absence of SecYEG and in the presence of YidC. This suggests that the polytopic MelB can be inserted with the help of YidC or by itself. Our *in vivo* experiments, however, do not reveal which other molecules, such as chaperones, may be involved in this insertion and folding process. Extending our previous *in vitro* insertion and folding experiments of another MFS member the lactose permease LacY,<sup>10</sup> we here observe that the fully unfolded and extracted MelB polypeptide cannot self-insert into the lipid membrane *in vitro*, even if YidC is present. Together with our previous finding that the fully unfolded and extracted LacY polypeptide can insert and fold into the membrane with the help of YidC,<sup>10</sup> our finding suggests that some MFS members such as MelB require additional molecules other than YidC to facilitate insertion. It has been suggested that the signal recognition particle (SRP) is involved in the co-translational targeting of the transmembrane domain and/or the flanking region of the membrane protein to the membrane.<sup>1,46</sup> However, other still unknown chaperones may also be involved in this insertion process. More research is required to identify these factors and link them to the insertion process of MelB and possibly other polytopic membrane proteins.

Once the initial thermodynamic energy barrier to insert the first structural segment of the N-terminal domain of MelB is overcome, we observe that the partially unfolded MelB polypeptide can insert and fold itself into the membrane at relatively high probability, possibly because of its short periplasmic loops. However, with increasing time, the misfolding events of MelB increase and the insertion of segments stagnates. It is unlikely that MelB can reach its native fold under these conditions. Importantly, YidC considerably suppresses the structural segments of MelB from misfolding and increases their insertion and folding rate 2-fold. Very similar trends were previously observed for LacY,<sup>9</sup> despite having a generally lower probability of inserting and folding itself into the membrane. Notably, in the presence of YidC the insertion and folding rate of LacY was approximately 3-fold higher compared to MelB. Thus, YidC chaperones support and catalyze the stepwise insertion and folding of unfolded polypeptides into the membrane. For MelB, in 15% of all cases, the insertion and folding process proceeded until it completed its native fold after 5 s.

Interestingly, the insertion and folding of MelB in the presence and absence of YidC follows a certain pattern. Structural segments at both terminal ends of the MelB polypeptide insert and fold at higher probability compared to structural segments neighboring the 31 aa long middle-loop C3. Although this middle-loop C3 is located in the cytoplasm and does not have to pass through the inner membrane to fold, the folding process of the MelB polypeptide seems to be frequently disrupted by the misfolding of structural regions adjacent to the middle-loop C3. Although the precise insertion and folding mechanism of YidC is not well understood, YidC clearly plays an important role in chaperoning and catalyzing the folding particularly of structural segment S4a. Intriguingly, segment S4a contains the weakly hydrophobic  $\alpha$ -helix VII, which is a common structural feature in members of the MFS.<sup>47,48</sup> YidC is known to facilitate the insertion of transmembrane segments with low hydrophobicity,<sup>49</sup> which could explain why YidC considerably increases the folding and decreases the misfolding probabilities of the weakly

hydrophobic  $\alpha$ -helix VII and therefore of structural segment S4a. YidC had a similar effect on  $\alpha$ -helix VII in LacY.<sup>9</sup> Therefore, the weakly hydrophobic  $\alpha$ -helix VII could potentially play an important role in the YidC-assisted folding process.

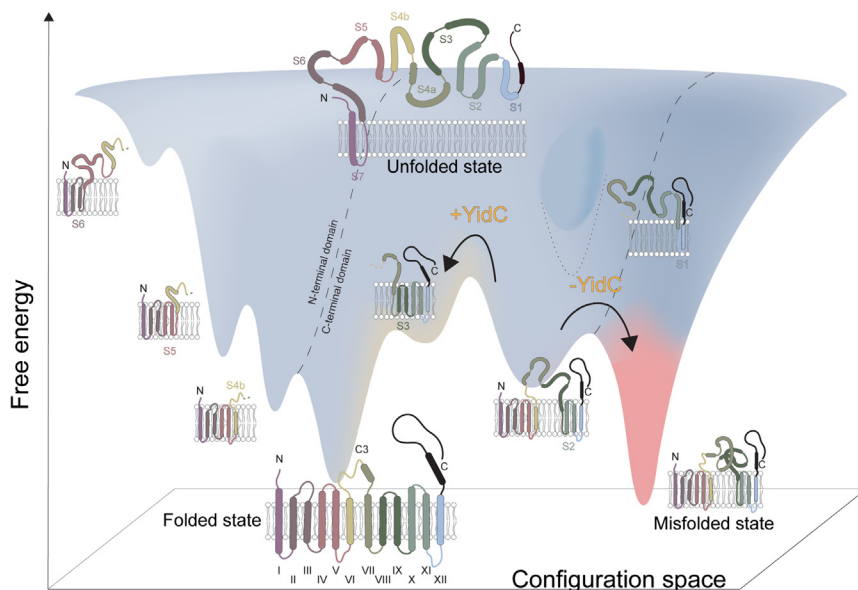
Our observation that the polytopic membrane protein MelB takes an intrinsic insertion and folding pathway of two simultaneously inserting and folding cores, one formed by the N-terminal domain and one by the C-terminal domain, is surprising. It may be supported by the *in vivo* experiment where the functional lactose permease LacY assembled from two separately expressed truncated C- and N-terminal domains.<sup>50</sup> So far, the formation of two or more independent folding cores of polypeptides has been mainly described for water soluble proteins,<sup>51</sup> while the formation of two folding cores, which are related to structural symmetries, has been suggested for membrane transporters.<sup>52,53</sup> However, here we show for the first time that a membrane transporter can simultaneously insert and fold structural segments from two different domains until the insertion and folding process has been completed. The consequence of our finding is that membrane protein folding pathways can be much more complex than thought. The results considerably expand our previously described observation that YidC supports LacY in inserting and folding structural segments into the membrane at random order.<sup>9</sup> The key to understanding this variability lies, perhaps, in the observation that membrane proteins show largely their own intrinsic insertion and folding pathways, rather than that these pathways are shaped by YidC. However, YidC is certainly more important to chaperone and catalyze the insertion and folding pathway that MelB chooses in the absence of misfolding.

In summary, our findings considerably expand previous discoveries of the YidC-assisted insertion of the lactose permease LacY by adding important mechanistic details on how YidC more generally assists the insertion and folding process of complex polytopic membrane proteins. After overcoming the initial thermodynamic energy barrier i.e., insertion of the first N-terminal structural segment, the pseudo-symmetric MelB alone inserts and folds N-terminal and C-terminal transmembrane  $\alpha$ -helices at higher probability, suggesting that the two N- and C-terminal domains have separate intrinsic insertion and folding capacities. In contrast,  $\alpha$ -helices neighboring the long middle-loop C3 that connects both domains have low probability of insertion and folding and a high probability of misfolding (Figure 7). Our data show that YidC particularly chaperones  $\alpha$ -helix VII against misfolding and, at the same time, catalyzes the insertion and folding to complete the native fold of MelB. One could thus hypothesize that this middle-loop region represents a spatial obstacle for MelB to insert and fold into the membrane and that YidC takes on a quality control role for the folding this region.

## STAR★METHODS

Detailed methods are provided in the online version of this paper and include the following:

- KEY RESOURCES TABLE
- RESOURCE AVAILABILITY
  - Lead contact
  - Materials availability



smoothens the free-energy landscape to increase reaction kinetics (not indicated). Labeled are structural segments S1–S7, the cytoplasmic middle-loop C3 and transmembrane  $\alpha$ -helices I–XII, as well as the C- and N-termini of MelB.

**Figure 7. Schematic free-energy landscape of the polytopic membrane transporter MelB in the absence and presence of the insertase YidC**

In the absence and presence of YidC, the unfolded MelB polypeptide inserts and folds structural segments from both the C-terminal and the N-terminal domain. This simultaneous insertion and folding via two folding cores progresses from the C-terminal and N-terminal ends until the structural segments located at the middle-loop C3 that connects both terminal domains, are trapped by misfolding (red). In the presence of YidC (+YidC) the insertion and folding process accelerates and misfolding is suppressed. Unfolded, folded and misfolded states of MelB are separated by free-energy barriers. Each free-energy well stabilizes an inserted and folded structural segment such as indicated by secondary structural models. YidC suppresses misfolding and lowers the free-energy barriers, especially for structural segments S3 and S4a, to fold into the native state. YidC also accelerates the insertion and folding of structural segments, which indicates that the insertase

- Data and code availability
- **EXPERIMENTAL MODEL AND STUDY PARTICIPANT DETAILS**
- **METHOD DETAILS**
  - Analysis of MelB by protease mapping
  - Expression and purification of MelB and YidC
  - Reconstitution of MelB and MelB/YidC into liposomes
  - FD-based AFM imaging
  - SMFS unfolding experiments
  - Complete un- and refolding of MelB polypeptides
  - Partial un-/refolding of MelB polypeptides
- **QUANTIFICATION AND STATISTICAL ANALYSIS**
  - SMFS unfolding data selection and analysis
  - Analysis of completely un-/refolded MelB
  - Analysis of partially un-/refolded MelB
  - Statistical analysis
  - Protein sequence analysis

#### SUPPLEMENTAL INFORMATION

Supplemental information can be found online at <https://doi.org/10.1016/j.str.2023.08.012>.

#### ACKNOWLEDGMENTS

We thank Jack Kuipers and Hans-Michael Kaltenbach for their help with the statistical analysis. This work was supported by the Swiss National Science Foundation by the NCCR Molecular Systems Engineering (Grant No. 182587) and supported by the National Institutes of Health (Grant R01GM122759 to L.G.).

#### AUTHOR CONTRIBUTIONS

G.N. performed protease mapping in depletion strains including the controls. N.B. performed expression and purification of YidC. H.P. performed MelB expression and purification, as well as protein reconstitution. S.M. recorded the AFM images. J.H. wrote Igor scripts and C.A. Python scripts for SMFS

data analysis. N.B. performed SMFS experiments and analyzed all data. N.B., A.K., L.G., and D.J.M. designed the study and wrote the manuscript. All authors contributed to the discussion and the writing of the manuscript.

#### DECLARATION OF INTERESTS

The authors declare no competing interests.

Received: June 5, 2023

Revised: July 22, 2023

Accepted: August 18, 2023

Published: September 13, 2023

#### REFERENCES

1. Hegde, R.S., and Keenan, R.J. (2022). The mechanisms of integral membrane protein biogenesis. *Nat. Rev. Mol. Cell Biol.* 23, 107–124. <https://doi.org/10.1038/s41580-021-00413-2>.
2. Driessen, A.J.M., and Nouwen, N. (2008). Protein translocation across the bacterial cytoplasmic membrane. *Annu. Rev. Biochem.* 77, 643–667. <https://doi.org/10.1146/annurev.biochem.77.061606.160747>.
3. Luirink, J., Yu, Z., Wagner, S., and de Gier, J.W. (2012). Biogenesis of inner membrane proteins in *Escherichia coli*. *Biochim. Biophys. Acta* 1817, 965–976. <https://doi.org/10.1016/j.bbabi.2011.12.006>.
4. Kuhn, A., Koch, H.G., and Dalbey, R.E. (2017). Targeting and Insertion of Membrane Proteins. *EcoSal Plus* 7. <https://doi.org/10.1128/ecosalplus.ESP-0012-2016>.
5. Oswald, J., Njenga, R., Natriashvili, A., Sarmah, P., and Koch, H.G. (2021). The Dynamic SecYEG Translocon. *Front. Mol. Biosci.* 8, e664241. <https://doi.org/10.3389/fmolb.2021.664241>.
6. Schulze, R.J., Komar, J., Botte, M., Allen, W.J., Whitehouse, S., Gold, V.A.M., Lycklama A Nijeholt, J.A., Huard, K., Berger, I., Schaffitzel, C., and Collinson, I. (2014). Membrane protein insertion and proton-motive-force-dependent secretion through the bacterial holo-translocon SecYEG–SecDF–YajC–YidC. *Proc. Natl. Acad. Sci. USA* 111, 4844–4849. <https://doi.org/10.1073/pnas.1315901111>.
7. Scotti, P.A., Urbanus, M.L., Brunner, J., de Gier, J.W., von Heijne, G., van der Does, C., Driessen, A.J., Oudega, B., and Luirink, J. (2000). YidC, the *Escherichia coli* homologue of mitochondrial Oxa1p, is a component of the

- Sec translocase. *EMBO J.* 19, 542–549. <https://doi.org/10.1093/emboj/19.4.542>.
8. Kiefer, D., and Kuhn, A. (2018). YidC-mediated membrane insertion. *FEMS Microbiol. Lett.* 365, 106. <https://doi.org/10.1093/femsle/fny106>.
  9. Serdiuk, T., Balasubramaniam, D., Sugihara, J., Mari, S.A., Kaback, H.R., and Müller, D.J. (2016). YidC assists the stepwise and stochastic folding of membrane proteins. *Nat. Chem. Biol.* 12, 911–917. <https://doi.org/10.1038/nchembio.2169>.
  10. Serdiuk, T., Mari, S.A., and Müller, D.J. (2017). Pull-and-Paste of Single Transmembrane Proteins. *Nano Lett.* 17, 4478–4488. <https://doi.org/10.1021/acs.nanolett.7b01844>.
  11. Nagamori, S., Smirnova, I.N., and Kaback, H.R. (2004). Role of YidC in folding of polytopic membrane proteins. *J. Cell Biol.* 165, 53–62. <https://doi.org/10.1083/jcb.200402067>.
  12. Anghel, S.A., McGilvray, P.T., Hegde, R.S., and Keenan, R.J. (2017). Identification of Oxa1 Homologs Operating in the Eukaryotic Endoplasmic Reticulum. *Cell Rep.* 21, 3708–3716. <https://doi.org/10.1016/j.celrep.2017.12.006>.
  13. Hennon, S.W., Soman, R., Zhu, L., and Dalbey, R.E. (2015). YidC/Alb3/Oxa1 Family of Insertases. *J. Biol. Chem.* 290, 14866–14874. <https://doi.org/10.1074/jbc.R115.638171>.
  14. Zhang, Y.-J., Tian, H.-F., and Wen, J.-F. (2009). The evolution of YidC/Oxa/Alb3 family in the three domains of life: a phylogenomic analysis. *BMC Evol. Biol.* 9, 137. <https://doi.org/10.1186/1471-2148-9-137>.
  15. Kumazaki, K., Kishimoto, T., Furukawa, A., Mori, H., Tanaka, Y., Dohmae, N., Ishitani, R., Tsukazaki, T., and Nureki, O. (2014). Crystal structure of *Escherichia coli* YidC, a membrane protein chaperone and insertase. *Sci. Rep.* 4, 7299. <https://doi.org/10.1038/srep07299>.
  16. Laskowski, P.R., Pluhackova, K., Haase, M., Lang, B.M., Nagler, G., Kuhn, A., and Müller, D.J. (2021). Monitoring the binding and insertion of a single transmembrane protein by an insertase. *Nat. Commun.* 12, 7082. <https://doi.org/10.1038/s41467-021-27315-3>.
  17. Chen, Y., Sotomayor, M., Capponi, S., Hariharan, B., Sahu, I.D., Haase, M., Lorigan, G.A., Kuhn, A., White, S.H., and Dalbey, R.E. (2022). A hydrophilic microenvironment in the substrate-translocating groove of the YidC membrane insertase is essential for enzyme function. *J. Biol. Chem.* 298, 101690. <https://doi.org/10.1016/j.jbc.2022.101690>.
  18. Klenner, C., and Kuhn, A. (2012). Dynamic Disulfide Scanning of the Membrane-inserting Pf3 Coat Protein Reveals Multiple YidC Substrate Contacts. *J. Biol. Chem.* 287, 3769–3776. <https://doi.org/10.1074/jbc.M111.307223>.
  19. Bowie, J.U. (2005). Solving the membrane protein folding problem. *Nature* 438, 581–589. <https://doi.org/10.1038/nature04395>.
  20. White, S.H., and Wimley, W.C. (1999). Membrane protein folding and stability: Physical principles. *Annu. Rev. Biophys. Biomol. Struct.* 28, 319–365. <https://doi.org/10.1146/annurev.biophys.28.1.319>.
  21. Harris, N.J., Pellowe, G.A., Blackholly, L.R., Gulaidi-Breen, S., Findlay, H.E., and Booth, P.J. (2022). Methods to study folding of alpha-helical membrane proteins in lipids. *Open Biol.* 12, 220054. <https://doi.org/10.1098/rsob.220054>.
  22. Kedrov, A., Ziegler, C., Janovjak, H., Kühlbrandt, W., and Müller, D.J. (2004). Controlled unfolding and refolding of a single sodium-proton antiporter using atomic force microscopy. *J. Mol. Biol.* 340, 1143–1152. <https://doi.org/10.1016/j.jmb.2004.05.026>.
  23. Kessler, M., Gottschalk, K.E., Janovjak, H., Müller, D.J., and Gaub, H.E. (2006). Bacteriorhodopsin Folds into the Membrane against an External Force. *J. Mol. Biol.* 357, 644–654. <https://doi.org/10.1016/j.jmb.2005.12.065>.
  24. Damaghi, M., Köster, S., Bippes, C.A., Yildiz, O., and Müller, D.J. (2011). One beta Hairpin Follows the Other: Exploring Refolding Pathways and Kinetics of the Transmembrane beta-Barrel Protein OmpG. *Angew. Chem., Int. Ed.* 50, 7422–7424. <https://doi.org/10.1002/anie.201101450>.
  25. Thoma, J., Bosshart, P., Pfreundschuh, M., and Müller, D.J. (2012). Out but not in: the large transmembrane  $\beta$ -barrel protein FhuA unfolds but cannot refold via  $\beta$ -hairpins. *Structure* 20, 2185–2190. <https://doi.org/10.1016/j.str.2012.10.006>.
  26. Serdiuk, T., Steudle, A., Mari, S.A., Manioglou, S., Kaback, H.R., Kuhn, A., and Müller, D.J. (2019). Insertion and folding pathways of single membrane proteins guided by translocases and insertases. *Sci. Adv.* 5, eaau6824–2548. <https://doi.org/10.1126/sciadv.aau6824>.
  27. Ethayathulla, A.S., Yousef, M.S., Amin, A., Leblanc, G., Kaback, H.R., and Guan, L. (2014). Structure-based mechanism for Na<sup>+</sup>/melibiose symport by MelB. *Nat. Commun.* 5, 3009. <https://doi.org/10.1038/ncomms4009>.
  28. Guan, L., and Hariharan, P. (2021). X-ray crystallography reveals molecular recognition mechanism for sugar binding in a melibiose transporter MelB. *Commun. Biol.* 4, 931. <https://doi.org/10.1038/s42003-021-02462-x>.
  29. Duong, F., and Wickner, W. (1997). Distinct catalytic roles of the SecYE, SecG and SecDFyajC subunits of preprotein translocase holoenzyme. *EMBO J.* 16, 2756–2768. <https://doi.org/10.1093/emboj/16.10.2756>.
  30. Kleinbeck, F., and Kuhn, A. (2021). Membrane Insertion of the M13 Minor Coat Protein G3p Is Dependent on YidC and the SecAYEG Translocase. *Viruses* 13, 1414. <https://doi.org/10.3390/v13071414>.
  31. Bassilana, M., and Gwizdek, C. (1996). In vivo membrane assembly of the *E. coli* polytopic protein, melibiose permease, occurs via a Sec-independent process which requires the protonmotive force. *EMBO J.* 15, 5202–5208. <https://doi.org/10.1002/j.1460-2075.1996.tb00905.x>.
  32. Blaimschein, N., Hariharan, P., Manioglou, S., Guan, L., and Müller, D.J. (2023). Substrate-binding guides individual melibiose permeases MelB to structurally soften and to destabilize cytoplasmic middle-loop C3. *Structure* 31, 58–67.e4. <https://doi.org/10.1016/j.str.2022.11.011>.
  33. Müller, D.J., and Engel, A. (2007). Atomic force microscopy and spectroscopy of native membrane proteins. *Nat. Protoc.* 2, 2191–2197. <https://doi.org/10.1038/nprot.2007.309>.
  34. Bustamante, C., Marko, J.F., Siggia, E.D., and Smith, S. (1994). Entropic elasticity of lambda-phage DNA. *Science* 265, 1599–1600. <https://doi.org/10.1126/science.8079175>.
  35. Kedrov, A., Janovjak, H., Sapra, K.T., and Müller, D.J. (2007). Deciphering Molecular Interactions of Native Membrane Proteins by Single-Molecule Force Spectroscopy. *Annu. Rev. Biophys. Biomol. Struct.* 36, 233–260. <https://doi.org/10.1146/annurev.biophys.36.040306.132640>.
  36. Serdiuk, T., Sugihara, J., Mari, S.A., Kaback, H.R., and Müller, D.J. (2015). Observing a Lipid-Dependent Alteration in Single Lactose Permeases. *Structure* 23, 754–761. <https://doi.org/10.1016/j.str.2015.02.009>.
  37. Engel, A., and Gaub, H.E. (2008). Structure and Mechanics of Membrane Proteins. *Annu. Rev. Biochem.* 77, 127–148. <https://doi.org/10.1146/annurev.biochem.77.062706.154450>.
  38. Kedrov, A., Krieg, M., Ziegler, C., Kuhlbrandt, W., and Müller, D.J. (2005). Locating ligand binding and activation of a single antiporter. *EMBO Rep.* 6, 668–674. <https://doi.org/10.1038/sj.embor.7400455>.
  39. Sapra, K.T., Besir, H., Oesterhelt, D., and Müller, D.J. (2006). Characterizing molecular interactions in different bacteriorhodopsin assemblies by single-molecule force spectroscopy. *J. Mol. Biol.* 355, 640–650. <https://doi.org/10.1016/j.jmb.2005.10.080>.
  40. Ge, L., Perez, C., Wacławska, I., Ziegler, C., and Müller, D.J. (2011). Locating an extracellular K<sup>+</sup>-dependent interaction site that modulates betaine-binding of the Na<sup>+</sup>-coupled betaine symporter BetP. *Proc. Natl. Acad. Sci. USA* 108, 890–898. <https://doi.org/10.1073/pnas.1109597108>.
  41. Bippes, C.A., Ge, L., Meury, M., Harder, D., Ucurum, Z., Daniel, H., Fotiadis, D., and Müller, D.J. (2013). Peptide transporter DtpA has two alternate conformations, one of which is promoted by inhibitor binding. *Proc. Natl. Acad. Sci. USA* 110, E3978–E3986. <https://doi.org/10.1073/pnas.1312959110>.
  42. Müller, D.J., Engel, A., Matthey, U., Meier, T., Dimroth, P., and Suda, K. (2003). Observing membrane protein diffusion at subnanometer resolution. *J. Mol. Biol.* 327, 925–930. [https://doi.org/10.1016/S0022-2836\(03\)00206-7](https://doi.org/10.1016/S0022-2836(03)00206-7).
  43. Mulvihill, E., Sborgi, L., Mari, S.A., Pfreundschuh, M., Hiller, S., and Müller, D.J. (2018). Mechanism of membrane pore formation by human

- gasdermin-D. *EMBO J.* 37, e98321. <https://doi.org/10.15252/embj.201798321>.
44. Luirink, J., von Heijne, G., Houben, E., and de Gier, J.W. (2005). Biogenesis of inner membrane proteins in *Escherichia coli*. *Annu. Rev. Microbiol.* 59, 329–355. <https://doi.org/10.1146/annurev.micro.59.030804.121246>.
  45. Cymer, F., Von Heijne, G., and White, S.H. (2015). Mechanisms of Integral Membrane Protein Insertion and Folding. *J. Mol. Biol.* 427, 999–1022. <https://doi.org/10.1016/j.jmb.2014.09.014>.
  46. Petriman, N.-A., Jauß, B., Hufnagel, A., Franz, L., Sachelaru, I., Drepper, F., Warscheid, B., and Koch, H.-G. (2018). The interaction network of the YidC insertase with the SecYEG translocon, SRP and the SRP receptor FtsY. *Sci. Rep.* 8, 578. <https://doi.org/10.1038/s41598-017-19019-w>.
  47. Bogdanov, M., Xie, J., Heacock, P., and Dowhan, W. (2008). To flip or not to flip: lipid-protein charge interactions are a determinant of final membrane protein topology. *J. Cell Biol.* 182, 925–935. <https://doi.org/10.1083/jcb.200803097>.
  48. Dowhan, W., and Bogdanov, M. (2009). Lipid-Dependent Membrane Protein Topogenesis. *Annu. Rev. Biochem.* 78, 515–540. <https://doi.org/10.1146/annurev.biochem.77.060806.091251>.
  49. Ernst, S., Schönbauer, A.K., Bär, G., Börsch, M., and Kuhn, A. (2011). YidC-Driven Membrane Insertion of Single Fluorescent Pf3 Coat Proteins. *J. Mol. Biol.* 412, 165–175. <https://doi.org/10.1016/j.jmb.2011.07.023>.
  50. Stochaj, U., Fritz, H.J., Heibach, C., Markgraf, M., von Schawen, A., Sonnewald, U., and Ehling, R. (1988). Truncated forms of *Escherichia coli* lactose permease: models for study of biosynthesis and membrane insertion. *J. Bacteriol.* 170, 2639–2645. <https://doi.org/10.1128/jb.170.6.2639-2645.1988>.
  51. Balchin, D., Hayer-Hartl, M., and Hartl, F.U. (2016). In vivo aspects of protein folding and quality control. *Science* 353, 4354. <https://doi.org/10.1126/science.aac4354>.
  52. Min, D., Jefferson, R.E., Qi, Y., Wang, J.Y., Arbing, M.A., Im, W., and Bowie, J.U. (2018). Unfolding of a ClC chloride transporter retains memory of its evolutionary history. *Nat. Chem. Biol.* 14, 489–496. <https://doi.org/10.1038/s41589-018-0025-4>.
  53. Choi, H.-K., Kang, H., Lee, C., Kim, H.G., Phillips, B.P., Park, S., Tumescheit, C., Kim, S.A., Lee, H., Roh, S.-H., et al. (2022). Evolutionary balance between foldability and functionality of a glucose transporter. *Nat. Chem. Biol.* 18, 713–723. <https://doi.org/10.1038/s41589-022-01002-w>.
  54. Fontaine, F., Fuchs, R.T., and Storz, G. (2011). Membrane Localization of Small Proteins in *Escherichia coli*. *J. Biol. Chem.* 286, 32464–32474. <https://doi.org/10.1074/jbc.m111.245696>.
  55. Steudle, A., Spann, D., Pross, E., Shanmugam, S.K., Dalbey, R.E., and Kuhn, A. (2021). Molecular communication of the membrane insertase YidC with translocase SecYEG affects client proteins. *Sci. Rep.* 11, 3940. <https://doi.org/10.1038/s41598-021-83224-x>.
  56. Klenner, C., Yuan, J., Dalbey, R.E., and Kuhn, A. (2008). The Pf3 coat protein contacts TM1 and TM3 of YidC during membrane biogenesis. *FEBS Lett.* 582, 3967–3972. <https://doi.org/10.1016/j.febslet.2008.10.044>.
  57. Guan, L., Nurva, S., and Ankeshwarapu, S.P. (2011). Mechanism of melibiose/cation symport of the melibiose permease of *Salmonella typhimurium*. *J. Biol. Chem.* 286, 6367–6374. <https://doi.org/10.1074/jbc.M110.206227>.
  58. Botfield, M.C., and Wilson, T.H. (1988). Mutations that simultaneously alter both sugar and cation specificity in the melibiose carrier of *Escherichia coli*. *J. Biol. Chem.* 263, 12909–12915.
  59. Winterfeld, S., Imhof, N., Roos, T., Bär, G., Kuhn, A., and Gerken, U. (2009). Substrate-Induced Conformational Change of the *Escherichia coli* Membrane Insertase YidC. *Biochemistry* 48, 6684–6691. <https://doi.org/10.1021/bi9003809>.
  60. Hariharan, P., Tikhonova, E., Medeiros-Silva, J., Jeucken, A., Bogdanov, M.V., Dowhan, W., Brouwers, J.F., Weingarth, M., and Guan, L. (2018). Structural and functional characterization of protein–lipid interactions of the *Salmonella typhimurium* melibiose transporter MelB. *BMC Biol.* 16, 85. <https://doi.org/10.1186/s12915-018-0553-0>.
  61. Müller, D.J., Amrein, M., and Engel, A. (1997). Adsorption of biological molecules to a solid support for scanning probe microscopy. *J. Struct. Biol.* 119, 172–188. <https://doi.org/10.1006/jsbi.1997.3875>.
  62. Pfreundschuh, M., Martinez-Martin, D., Mulvihill, E., Wegmann, S., and Müller, D.J. (2014). Multiparametric high-resolution imaging of native proteins by force-distance curve-based AFM. *Nat. Protoc.* 9, 1113–1130. <https://doi.org/10.1038/nprot.2014.070>.
  63. Butt, H.J., and Jaschke, M. (1995). Calculation of thermal noise in atomic force microscopy. *Nanotechnology* 6, 1–7. <https://doi.org/10.1088/0957-4484/6/1/001>.
  64. Bosshart, P.D., Casagrande, F., Frederix, P.L.T.M., Ratera, M., Bippes, C.A., Müller, D.J., Palacin, M., Engel, A., and Fotiadis, D. (2008). High-throughput single-molecule force spectroscopy for membrane proteins. *Nanotechnology* 19, 384014. <https://doi.org/10.1088/0957-4484/19/38/384014>.
  65. Kessler, M., and Gaub, H.E. (2006). Unfolding barriers in bacteriorhodopsin probed from the cytoplasmic and the extracellular side by AFM. *Structure* 14, 521–527. <https://doi.org/10.1016/j.str.2005.11.023>.
  66. Ritzmann, N., Manioglou, S., Hiller, S., and Müller, D.J. (2022). Monitoring the antibiotic darobactin modulating the  $\beta$ -barrel assembly factor BamA. *Structure* 30, 350–359.e3. <https://doi.org/10.1016/j.str.2021.11.004>.
  67. Kawamura, S., Gerstung, M., Colozo, A.T., Helenius, J., Maeda, A., Beerewinkel, N., Park, P.S.H., and Müller, D.J. (2013). Kinetic, energetic, and mechanical differences between dark-state rhodopsin and opsin. *Structure* 21, 426–437. <https://doi.org/10.1016/j.str.2013.01.011>.
  68. Thoma, J., Burmann, B.M., Hiller, S., and Müller, D.J. (2015). Impact of holdase chaperones Skp and SurA on the folding of  $\beta$ -barrel outer-membrane proteins. *Nat. Struct. Mol. Biol.* 22, 795–802. <https://doi.org/10.1038/nsmb.3087>.
  69. Altschul, S.F., Madden, T.L., Schäffer, A.A., Zhang, J., Zhang, Z., Miller, W., and Lipman, D.J. (1997). Gapped BLAST and PSI-BLAST: a new generation of protein database search programs. *Nucleic Acids Res.* 25, 3389–3402. <https://doi.org/10.1093/nar/25.17.3389>.
  70. Altschul, S.F., Wootton, J.C., Gertz, E.M., Agarwala, R., Morgulis, A., Schäffer, A.A., and Yu, Y.K. (2005). Protein database searches using compositionally adjusted substitution matrices. *FEBS J.* 272, 5101–5109. <https://doi.org/10.1111/j.1742-4658.2005.04945.x>.

STAR★METHODS

KEY RESOURCES TABLE

REAGENT or RESOURCE	SOURCE	IDENTIFIER
<b>Antibodies</b>		
Mouse Monoclonal Anti-polyHistidine	Sigma-Aldrich	#0000127269
<b>Bacterial and virus strains</b>		
<i>E. coli</i> MK6	Klenner et al., 2008 <sup>56</sup>	N/A
<i>E. coli</i> LR1655	Kleinbeck et al., 2021 <sup>30</sup> Fontaine et al., 2011 <sup>54</sup>	N/A
<i>E. coli</i> DW2	Botfield et al., 1988 <sup>58</sup>	N/A
<i>E. coli</i> C43(DE3)	Sigma-Aldrich	Cat# CMC0019
<b>Chemicals, peptides, and recombinant proteins</b>		
Ampicillin sodium salt	ThermoFisher Sci., Inc	Cat# BP1760
dodecyl-β-D-maltopyranoside (DDM)	Anatrace	Cat# D310
octyl- β-D-glucoside (OG)	Anatrace	Cat# O311
Melibiose	Millipore	Cat# 1.12240
<i>E. coli</i> polar lipid extract	Avanti Polar lipids	Cat# 100600P
30 μCi <sup>35</sup> S-L-methionine/cysteine	BioTrend	Cat# ARS-0110-5
<b>Deposited data</b>		
Codes for SMFS unfolding data import and analysis procedure	Blaimschein et al., 2023 <sup>32</sup>	<a href="https://doi.org/10.5281/zenodo.7268838">https://doi.org/10.5281/zenodo.7268838</a>
Codes for SMFS data alignment procedure	Ritzmann et al., 2022 <sup>66</sup>	<a href="https://doi.org/10.5281/zenodo.5647099">https://doi.org/10.5281/zenodo.5647099</a>
Datasets used for Figure 2	This work	<a href="https://doi.org/10.5281/zenodo.8227649">https://doi.org/10.5281/zenodo.8227649</a>
Datasets used for Figure 3	This work	<a href="https://doi.org/10.5281/zenodo.8227774">https://doi.org/10.5281/zenodo.8227774</a>
Datasets used for Figure 6	This work	<a href="https://doi.org/10.5281/zenodo.8246776">https://doi.org/10.5281/zenodo.8246776</a>
Datasets used for supplementary figures	This work	<a href="https://doi.org/10.5281/zenodo.8227593">https://doi.org/10.5281/zenodo.8227593</a>
Codes for refolding data analysis of the data published in this work	This work	<a href="https://doi.org/10.5281/zenodo.8152223">https://doi.org/10.5281/zenodo.8152223</a>
<b>Recombinant DNA</b>		
pK95 ΔAH/MelB <sub>ST</sub> /polyGly/CHis <sub>9</sub>	Blaimschein et al., 2023 <sup>32</sup>	N/A
pMS119/YidC/CHis <sub>10</sub>	Winterfeld et al., 2009 <sup>59</sup>	N/A
<b>Software and algorithms</b>		
DP Processing Software (Version spm-5.0.135)	JPK Instruments	<a href="https://www.jpk.com">https://www.jpk.com</a>
Igor Pro 8 (Version 8.03)	WaveMetrics, Inc.	<a href="https://www.wavemetrics.com">https://www.wavemetrics.com</a>
RStudio (Version 1.2.5042)	RStudio, Inc.	<a href="https://www.rstudio.com/">https://www.rstudio.com/</a>
Pymol (Version 2.5.2)	Schrodinger	<a href="http://www.pymol.org">http://www.pymol.org</a>
Prism (Version 9.2.0)	Graphpad Software	<a href="http://www.graphpad.com">http://www.graphpad.com</a>
Nanoscope Analysis software (version 1.8)	Bruker	<a href="http://nanoscaleworld.bruker-axs.com/nanoscaleworld/">http://nanoscaleworld.bruker-axs.com/nanoscaleworld/</a>
<b>Other</b>		
EmulsiFlex-C3	Avestin	<a href="http://www.avestin.com/emulsiflex-c3.htm">www.avestin.com/emulsiflex-c3.htm</a>
OMCL-RC800PSA cantilevers	Olympus	Cat# OMCL-RC800PSA
ScanAsyst Fluid+ cantilevers	Bruker Nano Inc.	Cat# ScanAsyst Fluid+

## RESOURCE AVAILABILITY

### Lead contact

Further information and requests for resources and reagents should be directed to and will be fulfilled by the lead contact, Daniel J. Müller ([daniel.mueller@bsse.ethz.ch](mailto:daniel.mueller@bsse.ethz.ch)).

### Materials availability

This study did not generate new unique reagents. Plasmids and bacterial strains in this study will be available upon request.

### Data and code availability

Data for Figure 2 was deposited on Zenodo at <https://doi.org/10.5281/zenodo.8227649>, for Figure 3 at <https://doi.org/10.5281/zenodo.8227774> and for Figure 6 at <https://doi.org/10.5281/zenodo.8246776>, and is publicly available as of the date of publication. The DOIs are listed in the [key resources table](#).

All supplementary data reported in this paper was deposited on Zenodo at <https://doi.org/10.5281/zenodo.8227593> and is publicly available as of the date of publication. The DOI is listed in the [key resources table](#).

All original code was deposited on Zenodo at <https://doi.org/10.5281/zenodo.8152223> and is publicly available as of the date of publication. The DOI is listed in the [key resources table](#).

Any additional information required to reanalyze the data reported in this paper is available from the [lead contact](#) upon request.

## EXPERIMENTAL MODEL AND STUDY PARTICIPANT DETAILS

*E. coli* MK6 and LR1655 were used to determine the insertion capability of MelB under culture conditions as described in [Method details](#).

## METHOD DETAILS

### Analysis of MelB by protease mapping

We used *E. coli* depletion strains MK6 (YidC)<sup>56</sup> or LR1655 (SecE). LR1655 is a derivative of the *E. coli* strain MG1655 where the chloramphenicol cassette has been removed by pCP20.<sup>30,54</sup> Overnight cultures of each depletion strain were grown in Luria Broth (LB) medium (10 g tryptone, 5 g yeast extract, 10 g NaCl in 1 l distilled water, pH 7.4, Sigma-Aldrich) containing 100  $\mu\text{l ml}^{-1}$  ampicillin (Sigma-Aldrich), 0.2% (w:v) arabinose and 0.4% (w:v) glucose at 37°C. Cells were washed twice with LB medium and diluted 1:50 in fresh LB medium containing either 0.4% glucose or 0.2% arabinose, respectively, and grown at 37°C until the cultures reached a OD<sub>600</sub> of 0.5. For each condition, a sample was precipitated with trichloroacetic acid (TCA) and analyzed by a Western blot to ensure the expression and depletion of YidC and SecE, respectively. For protease mapping, 1 ml of each exponentially growing culture was washed twice with M9 salt solution (39 mM Na<sub>2</sub>HPO<sub>4</sub>, 22 mM KH<sub>2</sub>PO<sub>4</sub>, 18 mM NH<sub>4</sub>Cl, 8 mM NaCl) and subsequently resuspended in M9 medium (39 mM Na<sub>2</sub>HPO<sub>4</sub>, 22 mM KH<sub>2</sub>PO<sub>4</sub>, 18 mM NH<sub>4</sub>Cl, 8 mM NaCl, 1 mM MgSO<sub>4</sub>, 0.1 mM CaCl<sub>2</sub>, 5  $\mu\text{g ml}^{-1}$  thiamine, 0.0005% ammonium ferric citrate) containing 18 amino acids (aa) but methionine/cysteine and supplemented with either 0.4% glucose or 0.2% arabinose, respectively. The cells were grown for 1 h at 37°C, pulse labelled with 30  $\mu\text{Ci } ^{35}\text{S-L-methionine/cysteine}$  for 3 min, then chilled and spun down and resuspended in 500  $\mu\text{l}$  spheroplast buffer (40% (w:v) sucrose, 33 mM Tris-HCl, pH 8), treated with 5  $\mu\text{g}$  lysozyme and 0.5 mM ethylenediaminetetraacetic acid (EDTA) and incubated on ice for 10 min. The generated spheroplasts were kept on ice and divided into three aliquots of 200  $\mu\text{l}$  each, where one was immediately treated with 10% (w:v) TCA, the second with 0.2 mg proteinase K (Sigma-Aldrich) and the third with 0.2 mg proteinase K and 1% (v:v) Triton-X-100 for 1 h on ice, followed by precipitation with 10% TCA.

The precipitated samples with TCA were washed with ice cold acetone, dried, resuspended with 50  $\mu\text{l}$  2% sodium dodecyl sulfate (SDS) and 100 mM Tris-HCl (pH 8) buffer and warmed (40°C) for 5 min. Then, 1 ml TEN-TX buffer (150 mM NaCl, 10 mM Tris-HCl pH 8, 1 mM EDTA, 1% Triton-X-100) and 30  $\mu\text{l}$  StaphA solution (USBiological Life Science, Swampscott) were added. The preclearing of the samples was carried out at 4°C on a rotary wheel for 1 h, the StaphA was spun down, and the supernatant was divided into three aliquots. An antibody was added to detect the His-tag (Anti-His, Sigma-Aldrich) and kept overnight at 4°C. The samples were then spun down, washed twice with 1 mL TEN-TX and once with TEN buffer (150 mM NaCl, 10 mM Tris-HCl, pH 8, 1 mM EDTA). SDS-PAGE sample buffer was added, warmed (40°C) for 5 min, spun down and applied on 12% SDS-PAGE. The labelled protein bands were detected by phosphorimaging.

### Expression and purification of MelB and YidC

The plasmid pK95 $\Delta$ AH/MelB<sub>ST</sub>/polyGly/CHis<sub>9</sub> encoding *S. typhimurium* MelB with a 42 aa polyGly linker and a 9xHis tag has previously been described.<sup>32,57</sup> Constitutive expression of MelB in *E. coli* DW2 cells,<sup>58</sup> membrane preparations, and cobalt-affinity chromatography purification using detergent dodecyl- $\beta$ -D-maltopyranoside (DDM, Anatrace) were carried out as described.<sup>27</sup> The purified MelB samples were dialyzed overnight against a buffer consisting of 20 mM Tris-HCl, pH 7.5, 100 mM NaCl, 0.01% (w:v) DDM, and 10% (v:v) glycerol.



pMS119 encoding for 10xHis-tagged YidC<sup>59</sup> was used in this study. YidC was expressed in *E. coli* strain C43(DE3) in Difco Luria Bertani medium (LB; Becton, Dickinson and Co.) supplemented with 100  $\mu\text{g ml}^{-1}$  ampicillin (Sigma-Aldrich). At an optical density  $\text{OD}_{600} \approx 0.6$ , cells were induced with 0.5 mM isopropyl  $\beta$ -D-1-thiogalactopyranoside (IPTG, Sigma-Aldrich) and grown for 2 h at 37°C, followed by 30 min incubation on ice. Cells were harvested by centrifugation (7,000 rcf, 10 min) and resuspended in YidC buffer (20 mM Tris-HCl, pH 7.5, 300 mM NaCl, 10% glycerol) supplemented with DNase I (Roche Diagnostics), 1 mM  $\text{MgCl}_2$  and protease inhibitor (Roche). Cells were passed through an EmulsiFlex-C3 (Avestin) three times and a pressure of 1,500 bar. Unbroken and broken cells were separated by centrifugation (17,000 rcf, 20 min), and subsequently cell membranes collected by ultracentrifugation (108,860 rcf, 90 min). Membranes were solubilized using 1% DDM in YidC buffer overnight at 4°C. Insolubilized material was removed by centrifugation (108,860 rcf, 30 min) before incubating YidC with  $\text{Ni}^{2+}$ -NTA beads (Macherey-Nagel) and 20 mM imidazole (Carl Roth GmbH & Co. KG) for 3 h at 4°C. The beads were then loaded into a gravity column and washed with YidC buffer containing 30 mM imidazole and 0.05% DDM to remove unbound material. YidC was eluted with 300 mM imidazole and concentrated in a centrifugal tube (size cut-off 50 kDa, Amicon Ultra, Merck Millipore Ltd.). To remove the imidazole and adjust the detergent concentration to 0.05%, buffer exchange was performed using size exclusion columns (Illustra NAP-5, Cytiva).

### Reconstitution of MelB and MelB/YidC into liposomes

Reconstitution of MelB into proteoliposomes was carried out using a dilution method at a protein to lipid ratio of 1:5 (w:w) as described.<sup>32,60</sup> *E. coli* polar lipid extract (Avanti Polar lipids) was prepared at 40  $\text{mg ml}^{-1}$  in 1.2% (w:v) octyl- $\beta$ -D-glucoside (OG, Anatrace). Co-reconstitution of MelB together with YidC in YidC buffer supplemented with 0.05% (w:v) DDM was carried out following the same protocol but using equimolar ratios of MelB and YidC to achieve a protein to lipid ratio of 1:5 (w:w). After three cycles of freeze-thaw-sonication steps, the MelB or MelB/YidC proteoliposomes were aliquoted and frozen in liquid nitrogen for storage at  $-80^\circ\text{C}$ .

### FD-based AFM imaging

MelB and co-reconstituted MelB/YidC proteoliposomes were diluted (1:100) in imaging buffer (20 mM Tris-HCl, pH 7.5, 100 mM KCl, nanopure water (18 M $\Omega$ m)) and adsorbed on freshly cleaved mica for 10 min at room temperature. After adsorption, the sample was gently washed with imaging buffer five times to remove non-adsorbed membranes.<sup>61</sup> FD-based AFM imaging of proteoliposomes was performed with a Nanoscope Multimode 8 (Bruker) operated in PeakForce tapping mode in imaging buffer at room temperature.<sup>62</sup> In FD-based AFM, the AFM cantilever approaches and retracts from the sample in a pixel-by-pixel manner while raster-scanning to record force-distance curves. In this way, the distance between the cantilever tip and the sample is measured for each pixel to estimate the height profile of the sample topography. The AFM was placed in a temperature-controlled acoustic isolation box and equipped with a 120  $\mu\text{m}$  piezoelectric J scanner and fluid cell. AFM topographs were recorded using cantilevers (ScanAsyst-Fluid+, Bruker Nano Inc.) having a nominal spring constant of 0.7  $\text{N m}^{-1}$ , a resonance frequency of  $\approx 150$  kHz in liquid, and a sharpened silicon tip with a nominal radius of  $\approx 2$  nm. To prevent damage to the ultra-sharp tip, cantilevers were calibrated by applying the thermal noise method before imaging.<sup>63</sup> AFM topographs were recorded by applying imaging forces of 100 – 120 pN at 2 kHz oscillation frequency, with a vertical oscillation amplitude of 30 nm and a resolution of 384  $\times$  384 pixels. Image post-processing and analysis were performed using the Nanoscope Analysis software v.1.8.

### SMFS unfolding experiments

For each SMFS experiment, a frozen aliquot of proteoliposomes was thawed and adsorbed to freshly cleaved mica in SMFS buffer (20 mM Tris-HCl, pH 7.5, 100 mM NaCl, 20 mM melibiose, nanopure water (18 M $\Omega$ m)) for 10 min and subsequently rinsed with proteoliposome-free SMFS buffer to remove loosely attached or non-adsorbed proteoliposomes. The sample was covered with SMFS buffer and a silicon disc to avoid evaporation. Protein containing lipid patches were localized by AFM imaging (NanoWizard II Ultra/NanoWizard II, JPK Instruments) in SMFS buffer at  $\approx 25^\circ\text{C}$  (Figures S1B and S1C). For each experimental day a new cantilever (OMCL-RC800PSA, Olympus) was used and calibrated in SMFS buffer before the experiment using the equipartition theorem.<sup>63</sup>

For membrane protein unfolding experiments, the cantilever tip was pushed onto the membrane with a force of 700 pN for 0.5 s and retracted 250 nm with a velocity of 700  $\text{nm s}^{-1}$ . Upon retraction, the deflection was recorded as force-distance curve. To avoid repeated SMFS measurements at the same position, the location was changed after each approach-retract cycle following a two-dimensional pattern (Figure S3H).

### Complete un- and refolding of MelB polypeptides

The recently introduced “Pull-and-Paste” method was applied to completely unfold and extract single membrane proteins from the membrane by SMFS and to position the unfolded polypeptide at another membrane location to study its insertion.<sup>10</sup> Briefly, MelB containing proteoliposomes, or MelB and YidC containing proteoliposomes were adsorbed to freshly cleaved mica. After a MelB was fully unfolded and extracted from the membrane, the cantilever tip was used to place the unfolded polypeptide in close proximity ( $\approx 10$  nm) to the membrane at another location. The distance between the cantilever tip and the membrane ensures that the tip cannot contact and attach another MelB from the membrane. After a specified time (0.5 – 5 s, as stated), which the polypeptide was given to insert and fold into the membrane, the AFM tip was retracted from the membrane to detect whether it had inserted and folded into the membrane. To detect the mechanical unfolding of the natively folded MelB as well as of the refolded MelB polypeptide, we analyzed the force-distance curves recorded during retracting the cantilever.

### Partial un-/refolding of MelB polypeptides

After applying a force of 700 pN for 0.5 s to the proteoliposomes to attach a MelB polypeptide to the tip of the cantilever, the cantilever was retracted 130 nm (unless otherwise stated) to partially unfold MelB. After a given folding time (0.5 – 5 s, as stated), the cantilever tip, and therefore the partially unfolded MelB polypeptide, was brought into close proximity to the membrane ( $\approx 10$  nm) to allow the insertion and folding of the unfolded polypeptide. The cantilever was then retracted a second time to detect which structural regions of MelB have inserted, folded, or misfolded. The recorded force–distance curves of the first and second retraction of the cantilever were analyzed to determine the inserted and folded or misfolded structural regions of MelB.

The cantilever tip can unspecifically attach to any exposed polypeptide chain of a membrane protein.<sup>64,65</sup> Pushing the cantilever onto the MelB membrane unspecifically attaches the C-terminal end of MelB with a probability of  $\approx 0.01\%$ . To increase this probability of attachment ten-fold ( $\approx 0.1\%$ ), a 42 aa long unstructured polyglycine (polyGly) extension was engineered to the C-terminal end.<sup>32</sup> The unspecific attachment of the MelB polypeptide to the cantilever tip is temporary and only lasts a few seconds before the polypeptide slips off. Consequently, the probability of performing a successful insertion or folding experiment decreases considerably with increasing folding times. Therefore, more than 10,000 single-molecule experiments were necessary to record one folding event of the unfolded MelB polypeptide. On average, this correlates to two or three successful folding events per experimental day and AFM. Consequently, 40 – 60 days were needed to complete one experimental insertion and folding condition.

## QUANTIFICATION AND STATISTICAL ANALYSIS

### SMFS unfolding data selection and analysis

Each recorded force–distance curve was first corrected for deflection sensitivity and force offset with the cantilever calibration value of the respective experimental day before being subjected to a coarse filtering for force above noise level and length. The contour lengths of the elongated MelB (526 aa  $\hat{=}$  190 nm) and YidC (559 aa  $\hat{=}$  200 nm) polypeptides were calculated by assuming an amino acid backbone length of 0.36 nm aa<sup>-1</sup>. Since the AFM tip can attach to any exposed amino acid along the polypeptide chain, we used a cutoff value of 130 nm for both proteins to ensure that only force–distance curves displaying a complete force peak pattern pass the filter. In a subsequent step, force–distance curves showing obvious artifacts such as lipid tethers, aggregates or similar were excluded from further analysis. Data selection was performed using the data processing software from the AFM manufacturer (version spm-5.0.135, JPK Instruments).

The selected force–distance curves from the SMFS unfolding experiments were analyzed as previously described.<sup>32</sup> Briefly, force–distance curves were aligned and superimposed in Igor Pro 8 (version 8.03, WaveMetrics, Inc.). Subsequently, the curves were transformed into force–contour length space using the worm-like chain (WLC) model<sup>34</sup> and baseline corrected with the last 10% of data points (zero force). The force–distance curves were then semi-automatically aligned by a Python script<sup>66</sup> and each force peak of every force–distance curve saved in a data frame. The data frame was imported into an R script to generate the contour length histogram and fitted with a Gaussian mixture model.<sup>67</sup> Each Gaussian curve determines the force peak probability, mean contour length, and standard deviation (in aa) of a force peak.

### Analysis of completely un-/refolded MelB

The initial data selection process for force–distance curves recorded during the first retraction of the AFM cantilever was identical to the ‘SMFS unfolding data selection’ described above. After the characteristic MelB force peak pattern was detected, the 100 force–distance curves recorded during the second retraction were analyzed for force peaks using Igor Pro 8 (version 8.03, WaveMetrics, Inc). For the co-reconstituted MelB and YidC proteoliposomes, the number of force–distance curves recorded during the second retraction were 100 or less in case of the detection of a YidC or non-identifiable force peak pattern. The unspecific and transient attachment of the protein to the cantilever tip is very short lived and does not sustain for many approach–retract cycles of the AFM cantilever.<sup>9,68</sup> We choose a cut-off value of 100 cycles to reduce the measurement of unspecific interactions.

### Analysis of partially un-/refolded MelB

Each recorded force–distance curve was corrected for deflection sensitivity with the cantilever calibration value of the respective experimental day and for the force offset. Subsequently, the force–distance curve recording the first retraction of the AFM cantilever was filtered for force peaks above the noise level using the AFM data processing software (version spm-5.0.135, JPK Instruments). Curves that passed this filter were horizontally shifted to match the WLC curves obtained from the force peak pattern of natively folded MelB (Figure 2). Experiments in which the initially recorded unfolding force peaks did not match the force peak pattern of natively folded MelB were excluded from further analysis. In the next step, the horizontal shift was applied to the force–distance curve recorded during the second retraction of the cantilever. Each force peak of every force–distance curve (first and second retraction) was fitted with the WLC model to determine the contour length. For each experiment, the force peak pattern of the second retraction was then compared with that of the first retraction. The classification of the force curves was performed as described in the Results and Figure S5.

### Statistical analysis

Due to the low throughput of AFM-based SMFS experiments (details given above) and to obtain solid statistical information, force–distance curves recorded over multiple days under the same experimental conditions were pooled. The standard error (s.e.) of

<0.05% (>95% confidence interval (CI)) was calculated with a Z-score of 1.96 (Figures 6 and S7). The difference between folded (F), misfolded (M) and unfolded (U) MelB in the absence and presence of YidC was statistically analyzed by calculating the  $p$ -values using a two-tailed Fisher's exact test in GraphPad Prism9 for each given time (0.5 – 5 s). Therefore, F was compared to M + U, M to F + U and U to F + M (Figure 6A, and Table S1). The difference between correctly folded and misfolded segments in the absence and presence of YidC was statistically analyzed by calculating  $p$ -values with an unpaired, parametric, two-tailed t-test in GraphPad Prism9 for each given time (0.5 – 5 s) (Figures 6B and 6C; Table S2). The linear regression with a 95% CI of folded MelB segments in the absence and presence of MelB was performed in GraphPad Prism9, which is equivalent to an Analysis of Covariance (ANCOVA). The statistical analysis of the folding or misfolding probabilities of individual segments of MelB in the absence and presence of YidC was determined by calculating the  $p$ -values using a two-tailed z-test (test of equal or given proportions (prop.test function)) with a 95% CI in RStudio (Figure S7; Table S3 and S4). Statistical analysis was performed using RStudio (version 1.2.5042) and GraphPad Prism (version 9.2.0).

### Protein sequence analysis

The multiple sequence alignment (Figure S2) of *E. coli* (NCBI accession number NP\_418161.1) and *S. typhimurium* (NCBI accession number AAL22701.1) YidC was performed with BLASTP<sup>69,70</sup> using the default algorithm settings (Expected threshold: 0.05; Word size: 3; Matrix: BLOSUM62; Gap costs: Existence 11, Extension 1; and Compositional adjustments: Conditional compositional score matrix adjustment).